Supporting Information for

Catalytic control of enzymatic fluorine specificity

Amy M. Weeks and Michelle C.Y. Chang*

Materials and Methods

Commercial Materials. Acetyl coenzyme A sodium salt, *n*-propionyl coenzyme A lithium salt, acetoacetyl coenzyme A sodium salt hydrate, butyryl coenzyme A lithium salt hydrate, coenzyme A hydrate, coenzyme A trilithium salt, anhydrous *N*, *N*-dimethylformamide (DMF), chloroacetic anhydride, cyanoacetic acid, 2-(*N*-morpholino)ethanesulfonic acid (MES), *N*-cyclohexyl-3-aminopropanesulfonic acid (CAPS), sodium hydroxide, trifluoroacetic acid (TFA), sodium fluoroacetate, oxalyl chloride (2 M in dichloromethane), fluoropyruvic acid sodium salt, [$^2H_6$]-acetic anhydride (99 atom % D), [$^2H_4$]-acetic acid (99 atom % D) , [$^2H_2$]-sulfuric acid (96-98 wt % in D_2O, 99.5 atom % D), 5,5′-dithiobis(2-nitrobenzoic acid) (DTNB), tris(hydroxymethyl) aminomethane hydrochloride (Tris-HCl), hydroxylamine hydrochloride, urea, iodoacetamide, and sodium citrate dihydrate were purchased from Sigma-Aldrich (St. Louis, MO). Bromoacetic anhydride, methanol, acetonitrile, 4-(2-hydroxyethyl)-1-piperazineethanesulfonic acid (HEPES), monosodium phosphate monohydrate, disodium phosphate heptahydrate, triethylamine, hydrogen peroxide, sodium chloride, trichloroacetic acid (TCA), hydrochloric acid, tris(2-carboxylethyl)phosphine hydrochloride (TCEP), acetone, and D-sucrose were purchased from Fisher Scientific (Pittsburg, PA). 3,3,3-Trifluoropropionyl chloride was purchased from SynQuest (Alachua, FL). Deuterium oxide (100%) (D_2O) was purchased from Cambridge Isotope Laboratories (Andover, MA). Sequencing-grade chymotrypsin was purchased from Promega (Madison, WI).

Measurement of non-enzymatic hydrolysis rates. Non-enzymatic hydrolysis rates were measured by diluting either fluoroacetyl-CoA or acetyl-CoA into 1 mL water adjusted to the appropriate pH with either buffer (100 mM MES, pH 5.5; 100 mM MES, pH 6.5; 100 mM HEPES, pH 7.5; 100 mM CAPS, pH 10; 100 mM CAPS, pH 11) or sodium hydroxide (pH 12, 13, and 13.6). For experiments at <pH 13, aliquots (50 μL) were removed by hand at various times and quenched by mixing with 25 μL 50% (v/v) TFA. For experiments at pH > 13, acyl-CoAs were mixed with water adjusted to the appropriate pH with sodium hydroxide using a KinTek Chemical Quench Flow Model RQF-3 and the reaction was stopped at various time points by mixing with 50% (v/v) TFA. The pH values of the reaction mixtures were measured immediately after acyl-CoA addition and after hydrolysis to ensure that the pH remained constant during the experiment. Quenched samples were analyzed by HPLC on an Agilent Eclipse XDB-C18 (3.5 μm, 3.0 × 150 mm) using a linear gradient from 50 mM sodium phosphate, 0.1% (v/v) TFA, pH 4.5 to methanol over 15 min at 0.6 mL/min with detection of CoA absorbance at 260 nm. Percent conversion was calculated based on the peak areas for the acyl-CoA and free CoA. Plots of CoA released versus time were fit as pseudo-first-order

reactions to the equation [CoA] = $k[S]_0t$, where k is the rate constant, $[S]_0$ is the initial acyl-CoA concentration, and t is time.

Synthesis of substrates. Solvents used in chemical synthesis were dried using a VAC Solvent Purifier System (Vacuum Atmospheres Company, Amesbury, MA) with the exception of anhydrous DMF, which was purchased from Sigma-Aldrich. HPLC purifications were performed using an Agilent Eclipse XDB-C18 column (9.4 x 250 mm, 5 μm) connected to an Agilent 1200 binary pump and Agilent G1315D diode-array detector (*Figure S10*). Except where noted, a linear gradient from 0.2% (v/v) aqueous TFA to 100% methanol at 3 mL/min was applied over 90 min. HPLC fractions were assayed for the desired compounds by liquid chromatography-mass spectrometry (LC-MS) using an Agilent 1290 binary pump coupled to an Agilent 6130 single-quadrupole electrospray ionization mass spectrometer. Fractions containing the desired compounds were pooled, methanol was removed on a rotary evaporator, and the pooled fractions were lyophilized. The lyophilizate was dissolved in water and acyl-CoAs were quantified by absorbance at 260 nm ($\varepsilon_{260\ nm}$ = 13,100 M^{-1} cm^{-1}). Acyl-CoA solutions were stored at -80°C until further use. High-resolution mass spectral analyses were performed at the QB3/Chemistry Mass Spectrometry Facility at the University of California, Berkeley. NMR spectra were collected at the College of Chemistry NMR Facility at the University of California, Berkeley. One-dimensional spectra were recorded on Bruker AV-600 or AVQ-400 NMR spectrometers at 298 K. Chemical shifts are expressed in parts per million (δ, ppm) downfield from tetramethylsilane (^1H, ^2H, and ^{13}C) or trichlorofluoromethane (^{19}F) and are referenced to the solvent signal. Heteronuclear multiple bond correlation (HMBC) experiments were performed on a Bruker AV-500 NMR spectrometer at 298 K (*Figure S10*). Numbering for acyl-CoAs and $^1H/^{13}C$ HMBC crosspeaks is shown below. For spectra acquired in 90% H_2O/ 10% D_2O, the solvent signal was suppressed by direct pre-saturation.

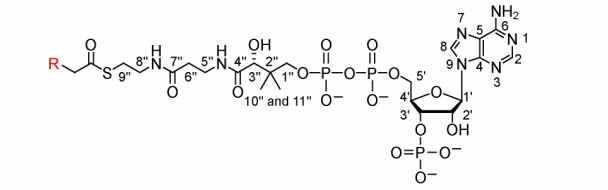

Crosspeak numbering for HMBC spectra

1	$H_{1''}C_{2''}$	10	$H_{10''}C_{11''}$	19	$H_{5''}C_{7''}$	28	H_2C_4
2	$H_{1''}C_{3''}$	11	$H_{10''}C_{2''}$	20	$H_{5''}C_{6''}$	29	H_2C_6
3	$H_{1''}C_{11''}$	12	$H_{10''}C_{1''}$	21	$H_{6''}C_{7''}$	30	H_8C_4
4	$H_{1''}C_{10''}$	13	$H_{10''}C_{3''}$	22	$H_{6''}C_{5''}$	31	H_8C_5
5	$H_{3''}C_{11''}$	14	$H_{11''}C_{10''}$	23	$H_{8''}C_{7''}$	32	$H_{1'}C_2$
6	$H_{3''}C_{10''}$	15	$H_{11''}C_{2''}$	24	$H_{8''}C_{9''}$	33	$H_{1'}C_4$
7	$H_{3''}C_{2''}$	16	$H_{11''}C_{1''}$	25	$H_{9''}C_{1RAc}$	34	$H_{1'}C_{4'}$
8	$H_{3''}C_{1''}$	17	$H_{11''}C_{3''}$	26	$H_{9''}C_{8''}$	35	$H_{2'}C_{1'}$
9	$H_{3''}C_{4''}$	18	$H_{5''}C_{4''}$	27	$H_{2RAc}C_{1RAc}$	36	$H_{3'}C_{4'}$

Fluoroacetyl-CoA (**1**) *(1, 2)*. Sodium fluoroacetate (100 mg, 1 mmol) was dried under vacuum for 12-16 h in a round-bottom flask equipped with a stir bar and a reflux condenser. The flask was placed under nitrogen pressure and dry tetrahydrofuran (2 mL), DMF (100 μL), and oxalyl chloride (2 M in dichloromethane, 500 μL) were added by syringe. The reaction mixture was heated to 65°C and stirred for 3-4 h. After cooling, 300 μL of the reaction mixture were added to a stirred, ice-cooled solution of coenzyme A hydrate (50 mg, ~0.06 mmol) and triethylamine (41.8 μL, 0.3 mmol) in DMF (1 mL). After 1 min, the reaction was quenched by addition of water (20 mL) and lyophilized. The lyophilizate was dissolved in water (1 mL) and purified three times by reverse-phase HPLC (0.022 mmol, 37%). ^{1}H NMR (600 MHz, D_2O, 25°C) δ (ppm): 8.45 (s, 1H, H_8), 8.28 (s, 1H, H_2), 6.03 (d, J = 6 Hz, 1H, $H_{1'}$), 4.87 (d, J = 46 Hz, C$\underline{H}_2$F), 4.73 (m, 2H, $H_{2'}$ and $H_{3'}$), 4.46 (s, 1H, $H_{4'}$), 4.16 (d, J = 15 Hz, 2H, $H_{5'}$), 3.86 (s, 1H, $H_{3''}$), 3.76 (m, 1H, $H_{1''}$), 3.55 (m, 1H, $H_{1''}$), 3.31 (t, J = 6 Hz, 2H, $H_{5''}$), 3.15 (t, J = 6 Hz, 2H, $H_{8''}$), 2.87 (t, J = 6.6 Hz, 2H, $H_{9''}$), 2.23 (t, J = 6.6 Hz , 2H, $H_{6''}$), 0.80 (s, 3H, $H_{10''}$), 0.69 (s, 3H, $H_{11''}$); ^{13}C NMR (150.9 MHz, D_2O, 25°C) δ (ppm): 199.86, 199.71 (FC$H_2\underline{C}$O), 174.54 ($C_{7''}$), 173.93 ($C_{4''}$), 149.65 (C_6), 148.29 (C_2), 144.69 (C_4), 142.34 (C_8), 118.31(C_5), 87.46 ($C_{1'}$), 85.41, 84.20 (F$\underline{C}H_2$CO), 82.95 ($C_{4'}$), 74.48 ($C_{2'}$), 74.45 ($C_{3''}$), 73.61 ($C_{3'}$), 72.24 ($C_{1''}$), 65.16 ($C_{5'}$), 38.31 ($C_{8''}$), 38.27 ($C_{2''}$) 35.38 ($C_{5''}$), 35.30 ($C_{6''}$), 26.87 ($C_{9''}$), 20.59 ($C_{10''}$), 18.31 ($C_{11''}$); ^{19}F NMR (564.7 MHz, D_2O, 25°C) δ (ppm): -226.1 (t, J = 49.2 Hz). HR-ESI-MS calcd (M-2H$^+$) *m/z* 412.5506, found (M-2H$^+$) *m/z* 412.5507.

Chloroacetyl-CoA (**7**) *(3)***.** Triethylamine (41.8 μL, 0.3 mmol) was added to an ice-cooled stirred solution of coenzyme A hydrate (50 mg, ~0.06 mmol) in DMF (1 mL). Chloroacetic anhydride (30.8 mg, 0.18 mmol) was added and the reaction mixture was stirred for 3 min at room temperature. The reaction was quenched by addition of water (20 mL) and lyophilized. The lyophilizate was dissolved in water (1 mL) and purified by reverse-phase HPLC (0.028 mmol, 47%). ^{1}H NMR (600 MHz, D_2O, 25°C) δ (ppm): 8.52 (s, 1H, H_8), 8.33 (s, 1H, H_2), 6.09 (d, J = 6 Hz, 1H, $H_{1'}$), 4.72 (m, 2H, $H_{2'}$ and $H_{3'}$), 4.50 (s, 1H, $H_{4'}$), 4.29 (s, 2H, C$\underline{H}_2$Cl), 4.21 (d, J = 13.8 Hz, 2H, $H_{5'}$), 3.92 (s, 1H, $H_{3''}$), 3.81 (m, 1H, $H_{1''}$), 3.59 (m, 1H, $H_{1''}$), 3.37 (t, J = 6.6 Hz, 2H, $H_{5''}$), 3.27 (t, J = 6.6 Hz, 2H, $H_{8''}$), 2.98 (t, J = 6 Hz, 2H, $H_{9''}$), 2.35 (t, J = 6.6 Hz , 2H, $H_{6''}$), 0.91 (s, 3H, $H_{10''}$), 0.80 (s, 3H, $H_{11''}$); ^{13}C NMR (150.9 MHz, D_2O, 25°C) δ (ppm): 197.25 (ClC$H_2\underline{C}$O), 174.58 ($C_{7''}$), 173.97 ($C_{4''}$), 149.70 (C_6), 148.33 (C_2), 144.70 (C_4), 142.37 (C_8), 118.36 (C_5), 87.46 ($C_{1'}$), 83.04 ($C_{4'}$), 74.42 ($C_{2'}$), 74.15 ($C_{3''}$), 73.66 ($C_{3'}$), 72.24 ($C_{1'}$), 65.15 ($C_{5'}$), 47.86 (Cl$\underline{C}H_2$CO), 38.34 ($C_{8''}$), 38.20 ($C_{2''}$) 35.33 ($C_{5''}$), 35.18 ($C_{6''}$), 28.60 ($C_{9''}$), 20.65 ($C_{10''}$), 18.32 ($C_{11''}$). HR-ESI-MS calcd (M-2H$^+$) *m/z* 420.5361, found (M-2H$^+$) *m/z* 420.5363.

Bromoacetyl-CoA (**6**) (*3*). Triethylamine (41.8 μL, 0.3 mmol) was added to an ice-cooled stirred solution of coenzyme A hydrate (50 mg, ~0.06 mmol) in DMF (1 mL). Bromoacetic anhydride (46.8 mg, 0.18 mmol) was added and the reaction mixture was stirred for 3 min at room temperature. The reaction was quenched by addition of water (20 mL) and lyophilized. The lyophilizate was dissolved in water (1 mL) and purified by reverse-phase HPLC (0.013 mmol, 21%). ^{1}H NMR (600 MHz, D_2O, 25°C) δ (ppm): 8.46 (s, 1H, H_8), 8.26 (s, 1H, H_2), 6.03 (d, J = 6 Hz, 1H, $H_{1'}$), 4.77 (m, 2H, $H_{2'}$ and $H_{3'}$), 4.51 (s, 1H, $H_{4'}$), 4.12 (d, J = 13.8 Hz, 2H, $H_{5'}$), 4.06 (s, 2H C$\underline{H}_2$Br), 3.90 (s, 1H, $H_{3'}$), 3.73 (m, 1H, $H_{1''}$), 3.49 (m, 1H, $H_{1''}$), 3.49 (t, J = 6.6 Hz, 2H, $H_{5''}$), 3.29 (t, J = 6.6 Hz, 2H, $H_{8''}$), 2.90 (t, J = 6.6 Hz, 2H, $H_{9''}$), 2.27 (t, J = 6.6 Hz , 2H, $H_{6''}$), 0.79 (s, 3H, $H_{10''}$), 0.66 (s, 3H, $H_{11''}$); ^{13}C NMR (150.9 MHz, D_2O, 25°C) δ (ppm): 196.39 (BrC$H_2\underline{C}$O), 174.61 ($C_{7''}$), 173.99 ($C_{4''}$), 149.74 (C_6), 148.38 (C_2), 144.67 (C_4), 142.39 (C_8), 118.36 (C_5), 87.45 ($C_{1'}$), 83.09 ($C_{4'}$), 74.39 ($C_{2'}$), 74.13 ($C_{3''}$), 73.67 ($C_{3'}$), 72.20 ($C_{1'}$), 65.11 ($C_{5'}$), 38.33 ($C_{8''}$), 38.20 ($C_{2''}$) 35.33 ($C_{5''}$), 35.19 ($C_{6''}$), 33.55 ($\underline{C}H_2$Br), 29.06 ($C_{9''}$), 20.68 ($C_{10''}$), 18.28 ($C_{11''}$). HR-ESI-MS calcd (M-2H$^+$) *m/z* 442.5106, found (M-2H$^+$) *m/z* 442.5105.

Cyanoacetyl-CoA (**8**)**.** Cyanoacetic acid (85 mg, 1 mmol) was dried under vacuum in an oven-dried round-bottom flask equipped with a stir bar. The flask was placed under nitrogen pressure and dry dichloromethane (2.4 mL), dry DMF (30 μL), and oxalyl chloride (600 μL, 2 M in dichloromethane) were added by syringe. The reaction mixture was stirred for 3 h at room temperature. A portion (150 μL) was then added to a stirred, ice-cooled solution of coenzyme A hydrate (50 mg, ~0.06 mmol) and triethylamine (41.8 μL, 0.3 mmol) in dry DMF (1 mL). After 1 minute, the reaction was quenched by addition of water (20 mL) and lyophilized. The lyophilizate was dissolved in water (1 mL) and purified by reverse-phase HPLC (0.005 mmol, 8.3%). The resonance corresponding to the α-protons of cyanoacetyl-CoA was not of the expected intensity when the ^{1}H NMR spectrum was recorded in D_2O. ^{1}H/^{13}C HMBC experiments verified that the peak had been assigned correctly, but also revealed the presence of the cyanoacetyl-CoA enolate tautomer (*Figure S10*). Comparison of the ^{1}H NMR spectrum of cyanoacetyl-CoA dissolved in D_2O to the spectrum of a sample dissolved in 90% H_2O/10% D_2O revealed that these protons readily exchange with solvent. ^{1}H NMR (600 MHz, 90% H_2O/10% D_2O, 25°C) δ (ppm): 8.50 (s, 1H, H_8), 8.28 (s, 1H, H_2), 6.06 (d, J = 5.4 Hz, 1H, $H_{1'}$), 4.74 (m, 2H, $H_{2'}$ and $H_{3'}$), 4.46 (s, 1H, $H_{4'}$), 4.13 (d, J = 10.8 Hz, 2H, $H_{5'}$), 3.88 (s, 1H, $H_{3''}$), 3.73 (m, 1H, $H_{1''}$), 3.58 (s, 2H, C$\underline{H}_2$CN), 3.49 (m, 1H, $H_{1''}$), 3.31 (t, J = 6 Hz, 2H, $H_{5''}$), 3.24 (t, J = 6 Hz, 2H, $H_{8''}$), 2.95 (t, J = 6 Hz, 2H, $H_{9''}$), 2.31 (t, J = 6.6 Hz , 2H, $H_{6''}$), 0.84 (s, 3H, $H_{10''}$), 0.68 (s, 3H, $H_{11''}$); ^{13}C NMR (150.9 MHz, D_2O, 25°C) δ (ppm): 191.26 (NCC$H_2\underline{C}$O), 174.68 ($C_{7''}$), 174.12 ($C_{4''}$), 149.90 (C_6), 148.48 (C_2), 144.73 (C_4), 142.54 (C_8), 118.58 (C_5), 114.87 ($\underline{C}$N), 87.59 ($C_{1'}$), 83.27 ($C_{4'}$), 74.38 ($C_{2'}$), 74.26 ($C_{3''}$), 73.78 ($C_{3'}$), 72.22 ($C_{1'}$), 65.18 ($C_{5'}$), 38.37 ($C_{8''}$), 38.19 ($C_{2''}$)

35.39 ($C_{5''}$), 35.28 ($C_{6''}$), 28.98 ($C_{9''}$), 28.97 ($\underline{C}H_2CN$), 20.76 ($C_{10''}$), 18.38 ($C_{11''}$). HR-ESI-MS calcd ($M+H^+$) *m/z* 835.1278, found ($M+H^+$) *m/z* 835.1278.

[$^2H_2$]-Fluoroacetyl-CoA (**9**). Fluoropyruvic acid sodium salt (857 mg, 6.7 mmol) was dissolved in D_2O (10 g, 9 mL) and [$^2H_2$]-sulfuric acid (1.4 mL) in an 80 mL microwave reaction vessel. The mixture was allowed to react at 120°C with 300 W microwave irradiation in a CEM Discover Labmate microwave reactor for 3 h. After cooling, the reaction mixture was extracted with anhydrous diethyl ether (10 × 10 mL). The ether was removed by rotary evaporator and the resultant [$^2H_2$]-fluoropyruvic acid was dissolved in D_2O (10 g, 9 mL) and [$^2H_2$]-sulfuric acid (0.5 mL) and reacted for an additional 3 h under the same conditions. The reaction mixture was extracted with anhydrous diethyl ether (10 × 10 mL) and the solvent was removed on a rotary evaporator to yield [$^2H_2$]-fluoropyruvic acid as a yellow oil (660 mg, 91%). A single resonance was observed in the ^{19}F NMR spectrum, indicating the absence of monodeuterated and undeuterated fluoropyruvic acid. [$^2H_2$]-Fluoropyruvic acid (650 mg, 6 mmol) was dissolved in water (30 mL) and the solution was carefully adjusted to pH 7 with 2 M NaOH. Hydrogen peroxide (9 mL of a 30% solution) was added and the mixture was stirred at room temperature for 12 h. The mixture was acidified with dilute sulfuric acid and extracted with diethyl ether (10 × 10 mL). The ether was removed on a rotary evaporator and the resultant [$^2H_2$]-fluoroacetic acid was dissolved in water (10 mL), carefully neutralized with 2 M NaOH and lyophilized to yield sodium [$^2H_2$]-fluoroacetate (100 mg, 1 mmol, 17%) as a white powder. A single resonance was observed in the ^{19}F NMR spectrum, indicating the absence of monodeuterated and undeuterated sodium fluoroacetate. [$^2H_2$]-Fluoroacetyl-CoA was synthesized from sodium [$^2H_2$]-fluoroacetate and coenzyme A using the same protocol followed for synthesis of undeuterated fluoroacetyl-CoA. The lyophilized crude product was dissolved in water (1 mL) and purified three times by reverse-phase HPLC (0.013 mmol, 21%). [$^2H_2$]-Fluoroacetyl-CoA was judged to be >97% dideuterated based on the ratio of peak areas for undeuterated, monodeuterated, and dideuterated fluoroacetyl-CoA in the ^{19}F NMR spectrum. ^1H NMR (600 MHz, D_2O, 25°C) δ (ppm): 8.45 (s, 1H, H_8), 8.26 (s, 1H, H_2), 6.03 (d, J = 6 Hz, 1H, $H_{1'}$), 4.77 (m, 2H, $H_{2'}$ and $H_{3'}$), 4.51 (s, 1H, $H_{4'}$), 4.13 (d, J = 12.6 Hz, 2H, $H_{5'}$), 3.83 (s, 1H, $H_{3''}$), 3.70 (m, 1H, $H_{1''}$), 3.52 (m, 1H, $H_{1''}$), 3.31 (t, J = 6.6 Hz, 2H, $H_{5''}$), 3.22 (t, J = 6 Hz, 2H, $H_{8''}$), 2.93 (t, J = 6.6 Hz, 2H, $H_{9''}$), 2.29 (t, J = 6.6 Hz , 2H, $H_{6''}$), 0.79 (s, 3H, $H_{10''}$), 0.67 (s, 3H, $H_{11''}$); ^2H NMR (92.1 MHz, D_2O, 25°C) δ (ppm): 5.0 (d, J = 34 Hz); ^{13}C NMR (150.9 MHz, D_2O, 25°C) δ (ppm): 199.98, 199.83 ($FCD_2\underline{C}O$), 174.61 ($C_{7''}$), 174.00 ($C_{4''}$), 149.74 (C_6), 148.39 (C_2), 144.68 (C_4), 142.41 (C_8), 118.44 (C_5), 87.49 ($C_{1'}$), 83.07, 83.04 ($F\underline{C}D_2CO$), 83.00 ($C_{4'}$), 74.46 ($C_{2'}$), 74.44 ($C_{3''}$), 73.64 ($C_{3'}$), 72.30 ($C_{1''}$), 65.14 ($C_{5'}$), 38.30 ($C_{8''}$), 38.27 ($C_{2''}$) 35.33 ($C_{5''}$), 35.17 ($C_{6''}$), 26.89 ($C_{9''}$), 20.64 ($C_{10''}$), 18.31 ($C_{11''}$); ^{19}F NMR

(564.7 MHz, D_2O, 25°C) δ (ppm): -227.2 (m, J_{DF} = 7.5 Hz). HR-ESI-MS calcd ($M\text{-}2H^+$) *m/z* 413.5576, found ($M\text{-}2H^+$) *m/z* 413.5574.

[$^2H_3$]-Acetyl-CoA (**10**). Triethylamine (41.8 μL, 0.3 mmol) was added to an ice-cooled stirred solution of coenzyme A hydrate (50 mg, ~0.06 mmol) in DMF (1 mL). [$^2H_6$]-Acetic anhydride (19 mg, 17 μL, 0.18 mmol) was added and the reaction mixture was stirred for 3 min at room temperature. The reaction was quenched by addition of water (20 mL) and lyophilized. The lyophilizate was dissolved in water (1 mL) and purified by reverse-phase HPLC (0.020 mmol, 33%). [$^2H_3$]-Acetyl-CoA was judged to be 99% deuterated based on the absence of a peak for the α-protons in the ^1H NMR spectrum. ^1H NMR (600 MHz, D_2O, 25°C) δ (ppm): 8.30 (s, 1H, H_8), 8.13 (s, 1H, H_2), 5.89 (d, *J* = 6 Hz, 1H, $H_{1'}$), 4.57 (m, 2H, $H_{2'}$ and $H_{3'}$), 4.31 (s, 1H, $H_{4'}$), 4.03 (d, *J* = 13.2 Hz, 2H, $H_{5'}$), 3.71 (s, 1H, $H_{3''}$), 3.58 (m, 1H, $H_{1''}$), 3.39 (m, 1H, $H_{1''}$), 3.16 (t, *J* = 6.6 Hz, 2H, $H_{5''}$), 3.03 (t, *J* = 6.6 Hz, 2H, $H_{8''}$), 2.66 (t, *J* = 5.4 Hz, 2H, $H_{9''}$), 2.14 (t, *J* = 6.6 Hz , 2H, $H_{6''}$), 0.72 (s, 3H, $H_{10''}$), 0.54 (s, 3H, $H_{11''}$); ^2H NMR (92.1 MHz, D_2O, 25°C) δ (ppm): 2.15; ^{13}C NMR (150.9 MHz, D_2O, 25°C) δ (ppm): 200.70 ($CD_3\underline{C}O$), 174.52 ($C_{7''}$), 173.83 ($C_{4''}$), 149.62 (C_6), 148.27 (C_2), 144.67 (C_4), 142.32 (C_8), 118.28 (C_5), 87.44 ($C_{1'}$), 82.89 ($C_{4'}$), 74.49 ($C_{2'}$), 74.46 ($C_{3''}$), 73.58 ($C_{3'}$), 72.27 ($C_{1'}$), 65.15 ($C_{5'}$), 38.44 ($C_{8''}$), 38.30 ($C_{2''}$) 35.30 ($C_{5''}$), 35.11 ($C_{6''}$), 29.31 (1:1:1 t, *J* = 78 Hz, $\underline{C}D_3$) 28.12 ($C_{9''}$), 20.58 ($C_{10''}$), 18.29 ($C_{11''}$). HR-ESI-MS calcd ($M\text{-}2H^+$) *m/z* 405.0645, found ($M\text{-}2H^+$) *m/z* 405.0646.

3,3,3-Trifluoropropionyl-CoA (**11**). 3,3,3-Trifluoropropionyl chloride (70 mg, 49 μL, 0.48 mmol) was added to a stirred solution of coenzyme A trilithium salt (50 mg, 0.06 mmol) and triethylamine (41.8 μL, 0.3 mmol) in water (1 mL). After 1 min, the reaction mixture was purified by HPLC using a linear gradient from 0-100% B over 30 min at 3 mL/min (A: H_2O, B: acetonitrile). Fractions were assayed for 3,3,3-trifluoropropionyl-CoA by LC-MS and were flash-frozen in liquid nitrogen and lyophilized (0.012 mmol, 20%). ^1H NMR (600 MHz, D_2O, 25°C) δ (ppm): 8.44 (s, 1H, H_8), 8.22 (s, 1H, H_2), 5.98 (d, *J* = 6 Hz, 1H, $H_{1'}$), 4.71 (m, 2H, $H_{2'}$ and $H_{3'}$), 4.42 (s, 1H, $H_{4'}$), 4.11 (d, *J* = 13.8 Hz, 2H, $H_{5'}$), 3.84 (s, 1H, $H_{3''}$), 3.72 (m, 1H, $H_{1''}$), 3.47 (q, *J* = 12 Hz, $C\underline{H}_2CF_3$), 3.46 (m, 1H, $H_{1''}$), 3.26 (t, *J* = 6 Hz, 2H, $H_{5''}$), 3.18 (t, *J* = 6 Hz, 2H, $H_{8''}$), 2.89 (t, *J* = 6 Hz, 2H, $H_{9''}$), 2.24 (t, *J* = 6 Hz , 2H, $H_{6''}$), 0.77 (s, 3H, $H_{10''}$), 0.65 (s, 3H, $H_{11''}$); ^{13}C NMR (150.9 MHz, D_2O, 25°C) δ (ppm): 193.06 ($CF_3CH_2\underline{C}O$), 174.62 ($C_{7''}$), 173.96 ($C_{4''}$), 149.68 (C_6), 148.31 (C_2), 144.78 (C_4), 142.30 (C_8), 118.27 (C_5), 87.37 ($C_{1'}$), 83.28 ($C_{4'}$), 74.24 ($C_{2'}$), 74.20 ($C_{3''}$), 73.67 ($C_{3'}$), 72.10 ($C_{1'}$), 65.10 ($C_{5'}$), 38.35 ($C_{8''}$), 38.20 ($C_{2''}$) 35.31 ($C_{5''}$), 35.18 ($C_{6''}$), 28.51 ($C_{9''}$), 20.75 ($C_{10''}$), 18.24 ($C_{11''}$). ^{19}F NMR (564.7 MHz, D_2O, 25°C): -62.17. HR-ESI-MS calcd ($M\text{-}H^+$) *m/z* 876.1045, found ($M\text{-}H^+$) *m/z* 876.1050.

Steady-state kinetic experiments. Steady-state kinetic experiments were performed using 5,5´-dithiobis-(2-nitrobenzoic acid) (DTNB) to detect release of free coenzyme A as described previously *(1)*. Enzymatic reactions were initiated by addition of FlK (5 nM – 10 μM) to reaction mixtures containing butyryl-CoA, propionyl-CoA, acetyl-CoA, acetoacetyl-CoA, bromoacetyl-CoA, chloroacetyl-CoA, fluoroacetyl-CoA, or cyanoacetyl-CoA. When included, sucrose was added to a final concentration of 30% (w/v) from a 60% (w/v) stock solution. Each rate was measured in triplicate. Kinetic parameters (k_{cat} and K_M) were determined by fitting the data to the equation $V_0 = V_{max}[S]/K_M + [S]$, where V_0 is the initial rate and [S] is the substrate concentration, using Origin 6.0 (OriginLab Corporation, Northampton, MA). Pseudo-first order rates of non-enzymatic hydrolysis under assay conditions were measured by monitoring CoA release in the absence of enzyme. Data were fit to the equation $[CoA] = k[S]_0t$, where k is the rate constant, $[S]_0$ is the initial acyl-CoA concentration, and t is time. Taft plots were constructed by plotting log k_{uncat} or log k_{cat} versus the Taft polar substituent constant σ* for the α-substituent of each acyl-CoA tested *(4, 5)*. Error bars shown on the plot for uncatalyzed hydrolysis represent the standard error for three measurements of the pseudo-first-order rate constants. Error bars shown on the plot for FlK-catalyzed hydrolysis are derived from the Michaelis-Menten fits of triplicate data sets. Taft plots were fit to the equation $\log k = \rho^*\sigma^*$, where ρ* is the polar sensitivity factor.

Rapid quench kinetic experiments. Pre-steady-state kinetic experiments were performed using rapid chemical quench followed by HPLC separation of coenzyme A from unhydrolyzed acyl-CoA. FlK (25-100 μM in 20 mM Tris-HCl, pH 7.6, 50 mM NaCl) was mixed with substrate (250-3000 μM in water) using a KinTek Chemical Quench Flow Model RQF-3. The reaction was stopped at various times by mixing with 50% (v/v) TFA to achieve a final concentration of 17% (v/v) TFA. Quenched samples were analyzed by HPLC on an Agilent Eclipse XDB-C18 (3.5 μm, 3.0 × 150 mm) using a linear gradient from 50 mM sodium phosphate, 0.1% (v/v) TFA, pH 4.5 to methanol over 15 min at 0.6 mL/min with detection of CoA absorbance at 260 nm. Percent conversion was calculated based on the peak areas for substrate and product. Plots of coenzyme A released versus time were fit to the equation $[CoA] = A^*(1-\exp(-k_2^*t)) + V^*t$, where A is the burst amplitude, k_2 is the burst-phase rate constant, and V is the steady-state rate. In cases where data could not be fit with a burst phase, they were fit as pseudo-first-order reactions according to the equation $[CoA] = k[FlK]t + [CoA]_0$, where the y-intercept, $[CoA]_0$, is the concentration of CoA released before the first data point, k is the rate constant, and t is time.

Hydroxylamine trapping of the acyl-enzyme intermediate. For trapping experiments with acetyl-CoA and fluoroacetyl-CoA, FlK (100 μM) in 20 mM Tris-HCl, pH 7.6, 50 mM NaCl (50 μL) was rapidly mixed with the appropriate substrate (acetyl-CoA, 6 mM; fluoroacetyl-CoA, 1

mM) using a KinTek Chemical Quench Flow Model RQF-3. The reaction was quenched after 300 ms (acetyl-CoA) or after 2 ms (fluoroacetyl-CoA) with 8 M urea in 50 mM citrate-phosphate buffer, pH 4.0 and collected into a tube containing 100 mM hydroxylamine in quench buffer. For trapping of the acyl-enzyme intermediate derived from 3,3,3-trifluoropropionyl-CoA, FlK (50 μM) in 20 mM Tris-HCl, pH 7.6, 50 mM NaCl (50 μL) was allowed to react with 3,3,3-trifluoropropionyl-CoA (1 mM) for 15 min. The reaction was quenched by the addition of 8 M urea in 50 mM citrate-phosphate buffer, pH 4.0 (450 μL) and 1 M hydroxylamine hydrochloride, pH 7.0 (50 μL). A control sample without any acyl-CoA substrate was also prepared following the same procedure. For all samples, FlK was precipitated by addition of 100% (w/v) trichloroacetic acid (125 μL). After standing on ice for 1 h, the sample was centrifuged at 20,817 × *g* for 10 min at 4°C to pellet the precipitated protein. The pellet was washed three times with ice cold 0.01 M HCl/90% acetone, air dried, and then dissolved in 100 mM Tris-HCl, pH 8.0, 8 M urea (80 μL). TCEP was added to a final concentration of 5 mM and the sample was incubated at room temperature for 20 min before adding iodoacetamide (10 mM final concentration) and incubating in the dark at room temperature for 15 min. The sample was then diluted with 100 mM Tris-HCl, pH 8.0 (720 μL) and sequencing-grade chymotrypsin (2 μg, Promega) was added. The digest was allowed to proceed overnight at room temperature and was then quenched by addition of formic acid to 5% (v/v). The sample was desalted on a C18 OMIX tip (Agilent). A nano LC column consisting of 10 cm of Polaris C18 5 μm packing material (Agilent) was packed into a glass capillary (100 μm inner diameter) using a pressure bomb. The column was extensively equilibrated with buffer A (5% acetonitrile/0.02% heptafluorobutyric acid (HFBA)) and directly coupled to an electrospray ionization source mounted on a Thermo-Fisher LTQ XL linear ion trap mass spectrometer. An Agilent 1200 HPLC equipped with a split line to deliver a flow rate of 30 nL/min was used for chromatography. Peptides were eluted using a gradient from 100% buffer A to 60% buffer B (80% acetonitrile/0.02% HFBA). The programs SEQUEST and DTASELECT *(6, 7)* were used to identify peptides from a database of the protein sequence and a database of common contaminants.

Phylogenetic analysis and sequence alignments. Representative sequences were retrieved from Pfam seed sequence sets from eight characterized families with the hotdog superfamily. The sequences, along with the sequences of FlK and its only known homolog with >60% sequence identity, were aligned using the PRALINE multiple sequence alignment server *(8)*, which incorporates information from PSI-BLAST pre-profile processing and PSIPRED secondary structure prediction. The alignment was manually adjusted where necessary to incorporate information from structural alignments. Using this alignment, a phylogenetic tree was constructed using the neighbor-joining method in MEGA 5 *(9)*. The bootstrap consensus tree

inferred from 500 replicates is taken to represent the evolutionary history of the 78 sequences analyzed. Bootstrap values are indicated next to the branches. The tree is drawn to scale in units of number of amino acid differences per site. There were a total of 37 positions in the final dataset.

Kinetic isotope effect measurements. Kinetic isotope effects were measured by direct comparison of the kinetic constants for α-deuterated and undeuterated substrates. Fluoroacetyl-CoA and [$^2H_2$]-fluoroacetyl-CoA were purified three times by HPLC. Acetyl-CoA purchased from Sigma-Aldrich and [$^2H_3$]-acetyl-CoA were both purified by reverse-phase HPLC to ensure similar sample composition. Steady-state kinetic experiments were performed by mixing equal volumes of FlK (120 nM in 20 mM Tris-HCl, pH 7.6, 50 mM NaCl for fluoroacetyl-CoA; 20 μM in 20 mM Tris-HCl, pH 7.6, 50 mM NaCl for acetyl-CoA) and deuterated or undeuterated substrate (10-200 μM in water for fluoroacetyl-CoA; 500-6000 μM for acetyl-CoA) using a KinTek Chemical Quench Flow Model RQF-3. The reactions were stopped at various points on the second timescale by mixing with 50% (v/v) TFA to achieve a final concentration of 17% (v/v) TFA. Quenched samples were analyzed by HPLC on an Agilent Eclipse XDB-C18 (3.5 μm, 3.0 × 150 mm) using a linear gradient from 50 mM sodium phosphate, 0.1% (v/v) TFA, pH 4.5 to methanol over 15 min at 0.6 mL/min with detection of CoA absorbance at 260 nm. Rates were determined by linear fitting of a plot of CoA released versus time using 12-15 data points for each substrate concentration. Error bars shown for individual rates represent the error derived from linear fitting. Kinetic constants were determined by fitting a plot of the initial rates (V_0) versus substrate concentration ([S]) to the equation $V_0 = V_{max}[S] / K_M + [S]$. Kinetic isotope effects were determined by calculating the ratios k_H/k_D and $^DV/K$. Errors for the individual parameters were propagated to calculate the errors for the kinetic isotope effect.

For pre-steady-state kinetic isotope effect experiments, FlK (50 μM in 20 mM Tris-HCl, pH 7.6, 50 mM NaCl) was mixed with deuterated or undeuterated substrate (500 μM in water) using the chemical quench flow apparatus and reactions were quenched by mixing with 50% (v/v) TFA. The plot of CoA released versus time for [$^2H_2$]-fluoroacetyl-CoA was best fit by the burst equation $[CoA] = A*(1-\exp(-k_2*t)) + V*t$, where A is the burst amplitude, k_2 is the burst-phase rate constant, and V is the steady-state rate. For undeuterated fluoroacetyl-CoA, the plot was best fit by a line.

Time-dependent fluoride release and FlK inactivation with 3,3,3-trifluoropropionyl-CoA.
FlK-catalyzed turnover of 3,3,3-trifluoropropionyl-CoA. Turnover of 3,3,3-trifluoropropionyl-CoA was measured using DTNB to detect release of free coenzyme A. Reactions were initiated

by addition of FlK to reaction mixtures containing 3,3,3-trifluoropropionyl-CoA (100, 250, 500, or 1000 μM) and DTNB (0.5 mM) in 20 mM Tris-HCl, pH 7.6, 50 mM NaCl. Time courses were fit to the equation [CoA] = A*(1-exp(-k_{obs}*t)) + V*t, where A is the concentration of CoA released during the first turnover of the reaction, k_{obs} is the rate constant for CoA release during the first turnover, and V is the rate for the pseudo-first-order phase of the reaction, which was found to correspond to the background rate of hydrolysis.

Inactivation of FlK by 3,3,3-trifluoropropionyl-CoA. Inactivation of FlK by 3,3,3-trifluoropropionyl-CoA was measured by testing the activity of FlK against fluoroacetyl-CoA at various time points after addition of 3,3,3-trifluoropropionyl-CoA. A solution of FlK (50 μM) was treated with 3,3,3-trifluoropropionyl-CoA (1 mM). At various time points after addition of 3,3,3,-trifluoropropionyl-CoA, an aliquot of the solution (0.5 μL) was removed and diluted 1:1000 into a reaction mixture containing fluoroacetyl-CoA (100 μM) and DTNB (0.5 mM) in 100 mM Tris-HCl, pH 7.6. Release of free coenzyme A was monitored by reaction of the thiol with DTNB. The rate constant for inactivation was measured by fitting a plot of activity remaining versus time after treatment with 3,3,3-trifluoropropionyl-CoA to the equation A = A_{final} + A_0*(1-exp(-k_{obs}*t)), where A is fraction of the initial activity remaining, A_{final} is the final activity, and A_0 is the initial activity.

FlK-catalyzed fluoride release from 3,3,3-trifluoropropionyl-CoA. Fluoride release was measured using a fluoride ion selective electrode (Mettler Toledo). FlK was dialyzed for 16 h against 2 L of 20 mM Tris-HCl, pH 7.6, 50 mM NaCl. The same dialysis buffer was then used for all subsequent protein and substrate dilutions and for dissolving sodium fluoride standards. FlK was diluted to 50 μM in dialysis buffer in total volume of 1 mL. Reactions were initiated by addition of 3,3,3-trifluoropropionyl-CoA (1 mM final concentration) and the change in fluoride electrode potential was recorded as a function of time. The background rate of fluoride release was measured by diluting 3,3,3-trifluoropropionyl-CoA to 1 mM in dialysis buffer in the absence of FlK. Electrode potential values were converted to fluoride concentration using a standard curve. The response time of the fluoride electrode was measured to be an order of magnitude faster than enzyme-catalyzed fluoride release (k_{obs} = 2 ± 0.1 min^{-1}). The background rate of fluoride release was subtracted and time courses of FlK-catalyzed fluoride release were fit to the equation [CoA] = A*(1-exp(-k_{obs}*t)) + F_0, where A is the final concentration of fluoride, k_{obs} is the rate constant, and F_0 is the initial amount of fluoride present in the solution.

Quantification of exchange of substrate α-protons with solvent. FlK storage buffer (20 mM Tris-HCl, pH 7.6, 50 mM NaCl) was prepared in H_2O and lyophilized. The buffer was dissolved

in D_2O and lyophilized a second time. The lyophilizate was dissolved in D_2O and used to equilibrate a Micro Bio-Spin column (Bio-Rad). A aliquot of concentrated FlK (50 μL) was passed over the column to exchange it into the deuterated solvent. A reaction mixture (1 mL) containing 3 mM acyl-CoA, 20 mM Tris-DCl, pD 7.6, 50 mM NaCl, and either 1 μM FlK (for fluoroacetyl-CoA) or 10 μM FlK (for acetyl-CoA) in D_2O was prepared. The reactions were allowed to proceed for 1 h at room temperature and were then lyophilized. The lyophilizate was dissolved in H_2O (200 μL) and analyzed by ^2H NMR (92.1 MHz, 25°C, 2000 scans) to look for deuterium exchange from solvent into the product α-protons. Standards containing either 150 μM [$^2H_3$]-acetic acid or 150 μM sodium [$^2H_2$]-fluoroacetate in the same buffer established that the limit of detection was <1%.

Supplementary Figures and Discussion

Figure S1. Alternative mechanisms for discrimination of fluoroacetyl-CoA and acetyl-CoA. (A) Fluoroacetyl-CoA could be discriminated based on carbonyl activation related to the fluorine substitution. In this model, the rate of nucleophilic attack on the fluorinated substrate is faster than the nonfluorinated substrate based on inductive effects that increase the electrophilicity at the carbonyl group. (B) Fluoroacetyl-CoA has the potential to form a hydrate or an enolate in aqueous solution, which could be the form of the substrate recognized by FlK. In this scenario, acetyl-CoA would bind poorly to the enzyme because it is less likely to form either the hydrate or enolate, allowing for specific hydrolysis of the fluorinated substrate. (C) $^{1}H/^{13}C$ HMBC spectrum of fluoroacetyl-CoA under FlK assay conditions. $^{1}H/^{13}C$ HMBC experiments show no evidence for formation of a fluoroacetyl-CoA hydrate or enolate within the limit of detection (see Materials and Methods for acyl-CoA numbering).

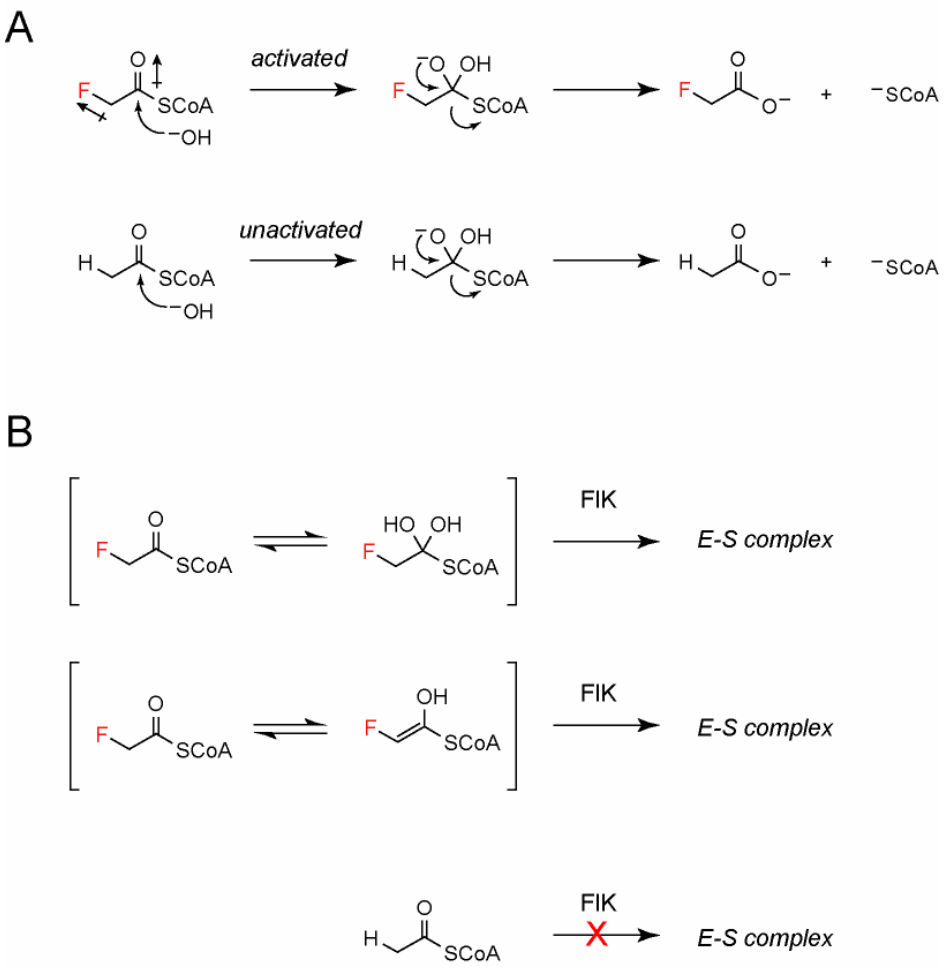

C

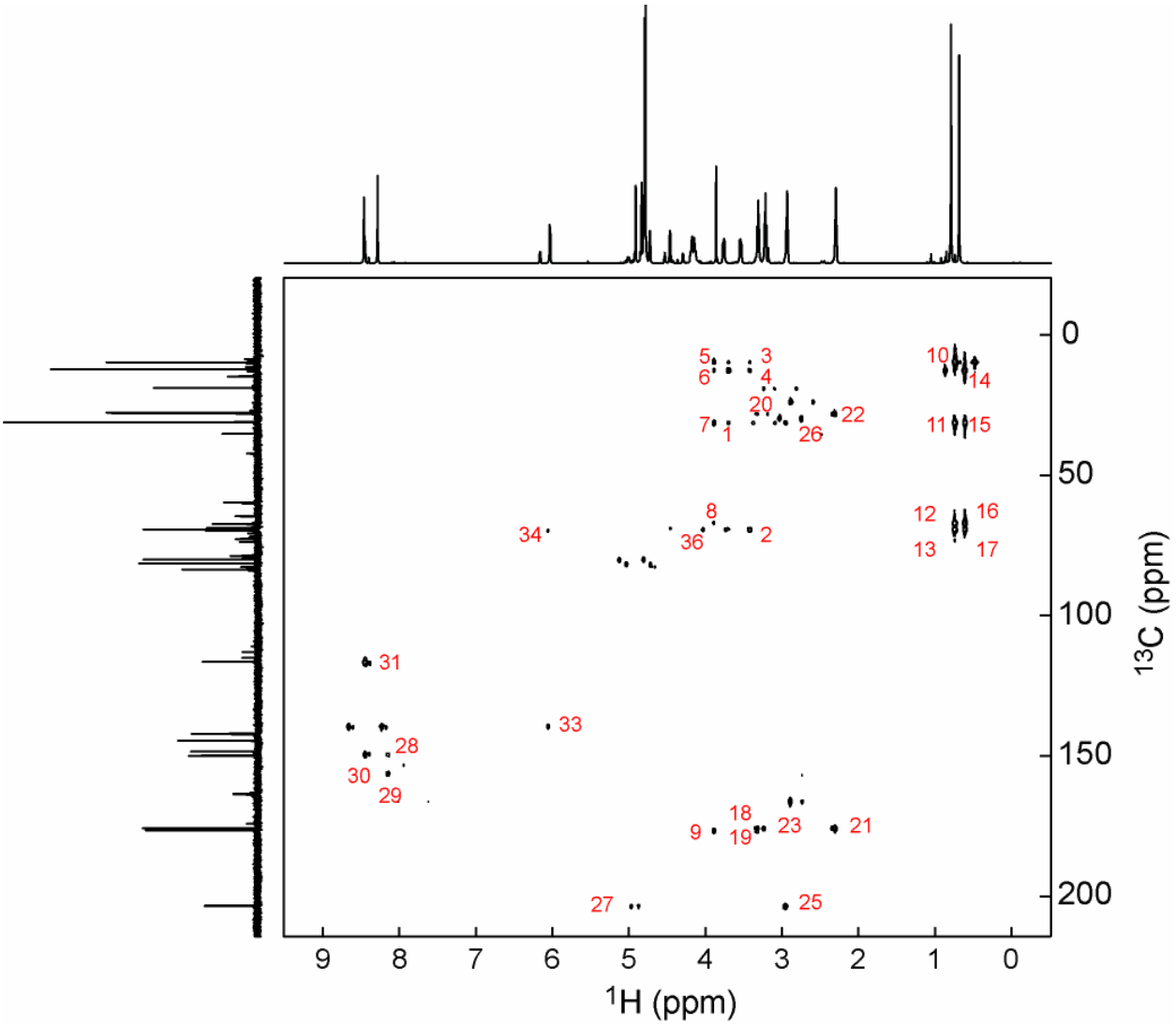
5
3
6
4
20
22
7
1
26
10
14
11
15
8
12
16
34
36
2
13
17
31
33
28
30
29
18
9
19
23
21
27
25
0
50
100
150
200
^{13}C (ppm)
9
8
7
6
5
4
3
2
1
0
^{1}H (ppm)

Figure S2. pH dependence of chemical hydrolysis rates of fluoroacetyl- and acetyl-CoA. (A) Ratios of rate constants for fluoroacetyl-CoA and acetyl-CoA hydrolysis. (B) Pseudo-first-order rate constants for fluoroacetyl-CoA and acetyl-CoA hydrolysis.

A

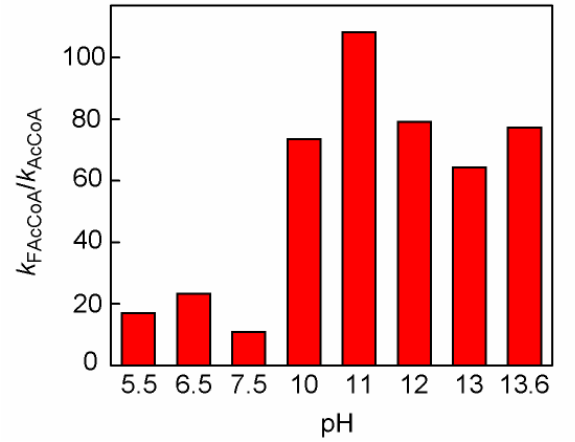

B

pH	k_{AcCoA} (s^{-1})	k_{FAcCoA} (s^{-1})
5.5	5.8×10^{-7}	9.8×10^{-6}
6.5	7.1×10^{-7}	1.6×10^{-5}
7.5	1.7×10^{-6}	1.8×10^{-5}
10	2.1×10^{-5}	1.5×10^{-3}
11	8.1×10^{-5}	8.8×10^{-3}
12	7.0×10^{-4}	4.0×10^{-1}
13	3.0×10^{-2}	8.0×10^{-1}
13.6	2.4×10^{-1}	5.1

SI Discussion. Taft analysis of acyl-CoA hydrolysis. Taft free-energy relationships were used to examine the sensitivity of FlK-catalyzed thioester hydrolysis to the electron-withdrawing ability of the α-substituent for a series of acyl-CoAs. The polar substituent constant (σ*) is derived from comparison of the rates of base-catalyzed hydrolysis of a series of methyl esters to the rates of acid-catalyzed hydrolysis of the same esters to separate and quantify steric and electronic effects *(4)*. The methyl group is defined as the reference substituent and its σ* is defined as 0. A linear relationship between σ* and the logarithm of the rate constant indicates that a consistent amount of charge accumulates in the transition state for all substituents, while an abrupt change in the slope of the plot indicates a change in the amount of charge buildup, suggesting a change in rate-determining step, chemical mechanism, or both. The slope of the line, ρ*, is the polar sensitivity factor that compares the reaction under study to the reference reaction. A slope >1 indicates that the reaction is more sensitive to substituents than the reference reaction, while a slope <1 indicates that it is less sensitive. Our analysis gave a ρ* value of 1.06 (R^2 = 0.99) for uncatalyzed hydrolysis and an ρ* of 2.3 (R^2= 0.98) for catalyzed hydrolysis, excluding fluoroacetyl-CoA and chloroacetyl-CoA from the linear fit.

Figure S3. Michaelis-Menten curves for substrates used in Taft analysis. (A) Butyryl-CoA. (B) Propionyl-CoA. (C) Acetyl-CoA. (D) Acetoacetyl-CoA. (E) Bromoacetyl-CoA. (F) Chloroacetyl-CoA. (G) Fluoroacetyl-CoA. (H) Cyanoacetyl-CoA.

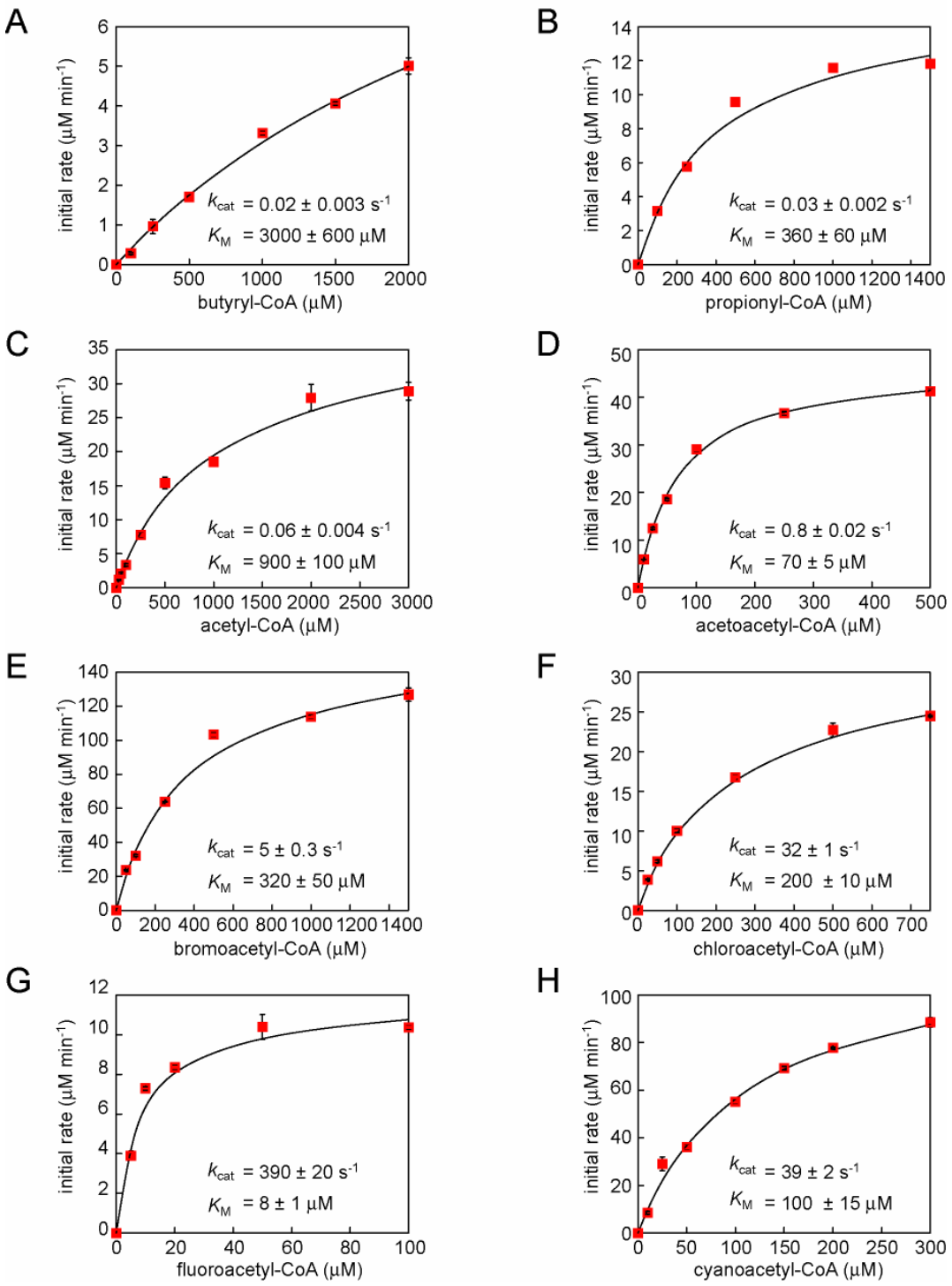

Figure S4. Characterization of FlK burst-phase kinetics. (A) Possible pathways of reaction between hydroxylamine and the acyl-anhydride intermediate. (B) LC-MS/MS analysis of hydroxylamine-quenched FlK reacted with acetyl-CoA showing the modification of the chymotryptic peptide containing Glu 50. (C) No modification was observed with FlK treated with hydroxylamine in the absence of acetyl-CoA substrate. Expected mass-to-charge (*m/z*) ratios for *b*-ions/y-ions are indicated. (D) Michaelis-Menten curve for FlK-catalyzed hydrolysis of acetyl-CoA in the presence (black) and absence (red) of sucrose. (E) Michaelis-Menten curve for FlK-catalyzed hydrolysis of fluoroacetyl-CoA in the presence (black) and absence (red) of sucrose. (F) Steady-state kinetic parameters for FlK in the presence and absence of sucrose.

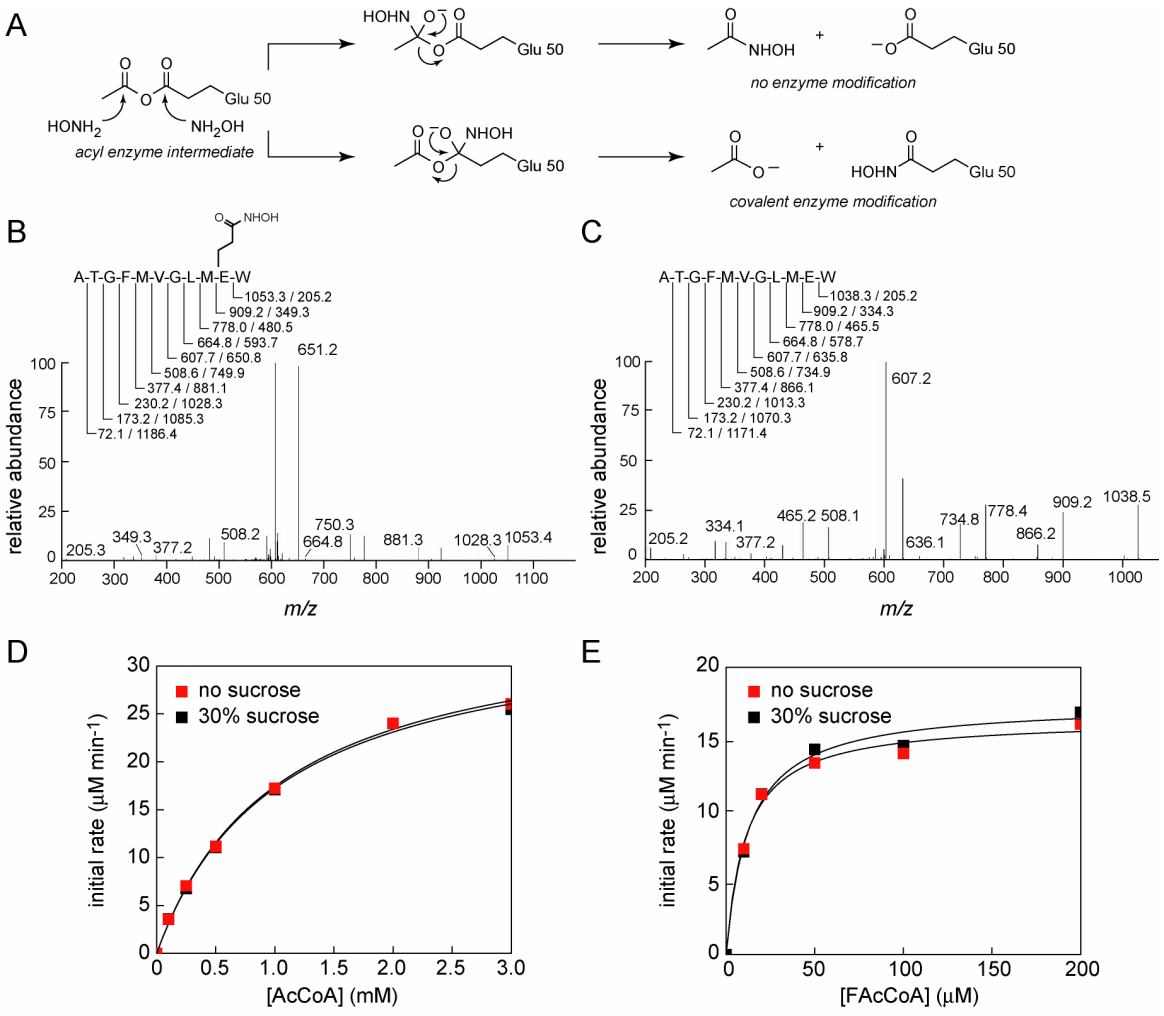

F

	% sucrose	k_{cat} (s^{-1})	K_M (µM)	k_{cat}/K_M ($M^{-1}s^{-1}$)
acetyl-CoA	0	0.06 ± 0.002	1040 ± 80	60 ± 5
	30	0.06 ± 0.002	1030 ± 80	60 ± 5
fluoroacetyl-CoA	0	219 ± 8	11 ± 2	(2.0 ± 0.4) x 10^7
	30	233 ± 8	13 ± 2	(1.8 ± 0.2) x 10^7

SI Discussion. Interpretation of pre-steady-state kinetic data. By quenching FlK-catalyzed hydrolysis reactions on a millisecond timescale, it is possible to monitor the rate of CoA release before the first turnover for many of the substrates used in Taft analysis. For fluoroacetyl-CoA hydrolysis, plots of CoA released versus time cannot be fit by the burst equation, but are best described by a linear fit. The earliest time at which our instrument is able to quench, however, is 2 ms, leaving open the possibility that FlK does have a burst phase with respect to fluoroacetyl-CoA, but it occurs with a rate constant of >500 s^{-1} and would therefore be over before the first quenched point that we are able to examine. To distinguish between the absence of a burst phase and the presence of a burst phase that is too fast to be measured by our assay, we examined the amount of free CoA present in the first quenched sample. If no burst phase had occurred, we would expect the CoA concentration to be given by [CoA] = k_{cat}[FlK]t, corresponding to a line with a y-intercept of zero. If a burst phase had occurred before the first quenched point, we would expect [CoA] = k_{cat}[FlK]t + [FlK], corresponding to a line with a y-intercept of [FlK]. For experiments conducted at three different FlK concentrations (25 μM, 50 μM, and 75 μM), we found that the data were best fit by lines whose y-intercepts were within error of zero. We therefore concluded that a step prior to or concomitant with CoA release is rate-limiting in the case of fluoroacetyl-CoA.

SI Discussion. Structural and functional comparison of FlK to PhaJ. Our phylogenetic analysis places FlK in closer evolutionary proximity to dehydratases than thioesterases. At the structural level, the similarities between FlK and the MaoC dehydratases are apparent. Structural alignment of FlK *(1, 10)* and the (*R*)-specific enoyl-CoA hydratase (PhaJ) from *Aeromonas caviae (11)* shows that the overall folds of the two enzymes are very similar, with a core rmsd of 1.7 Å. The alignment shows the presence of an 'overhanging segment' or lid that covers the active site and closes it off from solvent in both enzymes, although this feature had previously been considered to distinguish the MaoC family from other hot dog families *(11)*. In both enzymes, the lid is functionally important. In PhaJ, it encompasses the hydratase 2 motif that contains the catalytic Asp and His, while in FlK, the lid contains the Phe 33-Phe 36 gate, which closes the active site off from solvent and is involved in substrate affinity *(1)*.

The active sites of PhaJ and FlK also share many key features. Both are mainly hydrophobic, with the exception of the catalytic residues, and both are able to accommodate short-chain acyl-CoAs. PhaJ's catalytic triad consists of Asp 31, His 36, and Ser 62 *(11)*, while FlK's catalytic triad consists of Thr 42, Glu 50, and His 76 *(1)*. The Asp/Glu-His-Ser/Thr catalytic triad is common among many thioesterase and dehydratase members of the hot dog superfamily, and is often spatially permuted within the active site even between members with similar catalytic activities and chemical mechanisms. Site-directed mutagenesis studies of PhaJ and FlK demonstrate that mutation of the catalytic His to Ala leads to a 10^4-10^5-fold decrease in k_{cat} *(11)*, while mutation of the catalytic His in hot dog-fold thioesterases tends to have a smaller (2-4000-fold) impact *(12, 13)*. Mutation of the catalytic Asp/Glu affects thioesterases and dehydratases similarly *(1, 11-13)*, leading to a 10^4-10^5-fold decrease in k_{cat}. Mutation of Ser 62 in PhaJ and Thr 42 in FlK to Ala have similar impacts on catalytic activity (100-fold decrease in k_{cat}), and both residues have been proposed to be involved in positioning the other catalytic residues *(1, 11)*.

Figure S5. Phylogenetic and structural analysis of FlK homologs. (A) Uncompressed phylogenetic tree for FlK. An alignment of Pfam seed sequences from each family within the hot dog clan was performed using PRALINE. A neighbor-joining tree was then constructed in MEGA 5.0 and tested with 500 bootstrap replicates. Bootstrap values are listed near each branch. InterPro accession numbers are listed in parentheses.

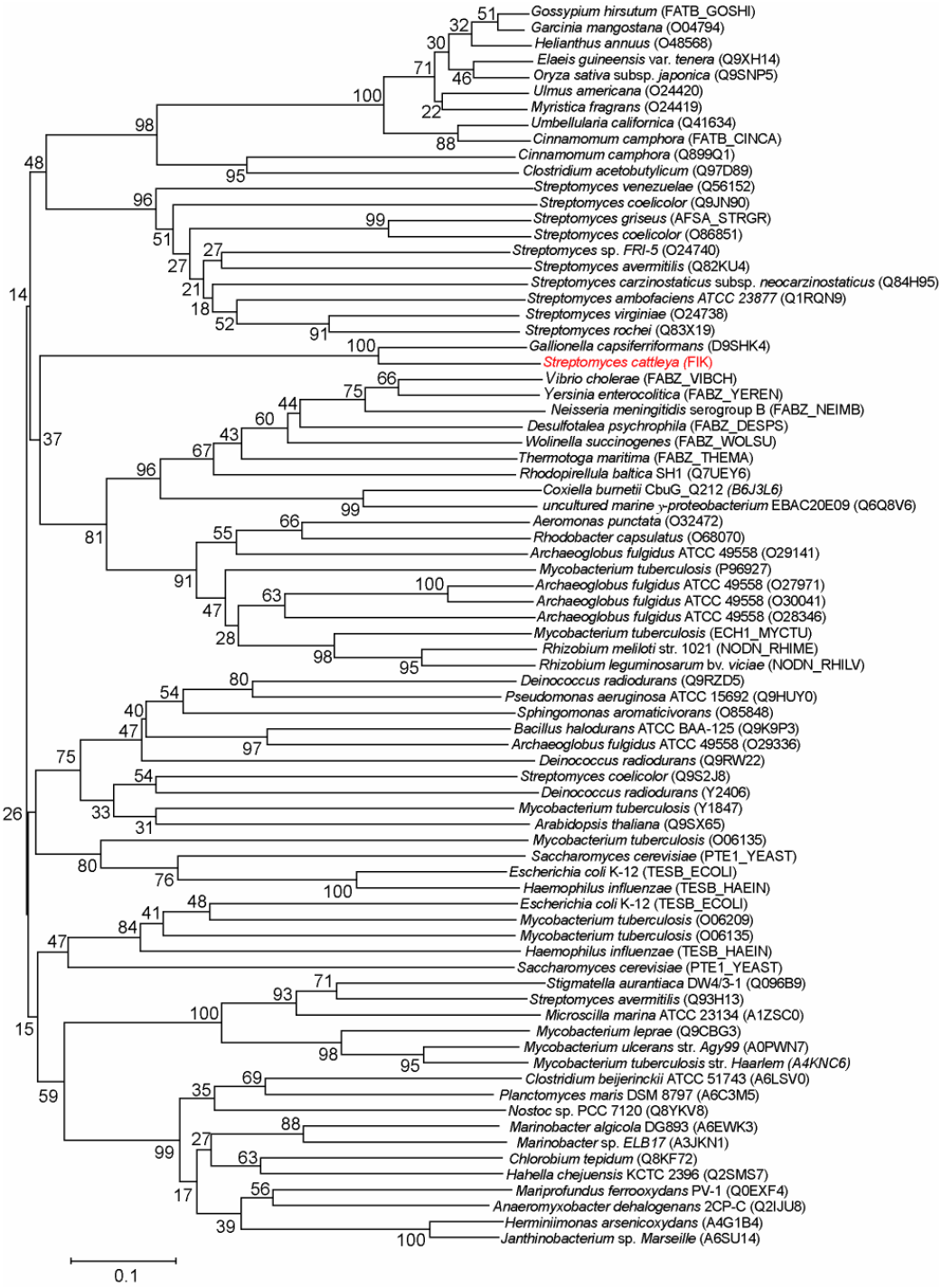

Figure S5B. Structural comparison of FlK to PhaJ. Overall folds of FlK showing lid (top left; PDB ID: 3P2Q) and PhaJ showing overhanging segment (top right; PDB ID: 1IQ6). A structural alignment of FlK and PhaJ (bottom) was performed by secondary structure matching using Coot *(14)* and shows a conserved phenylalanine in both the FlK lid and the PhaJ overhanging segment (FlK, light blue, Phe 36 magenta; PhaJ, navy, Phe 41, magenta).

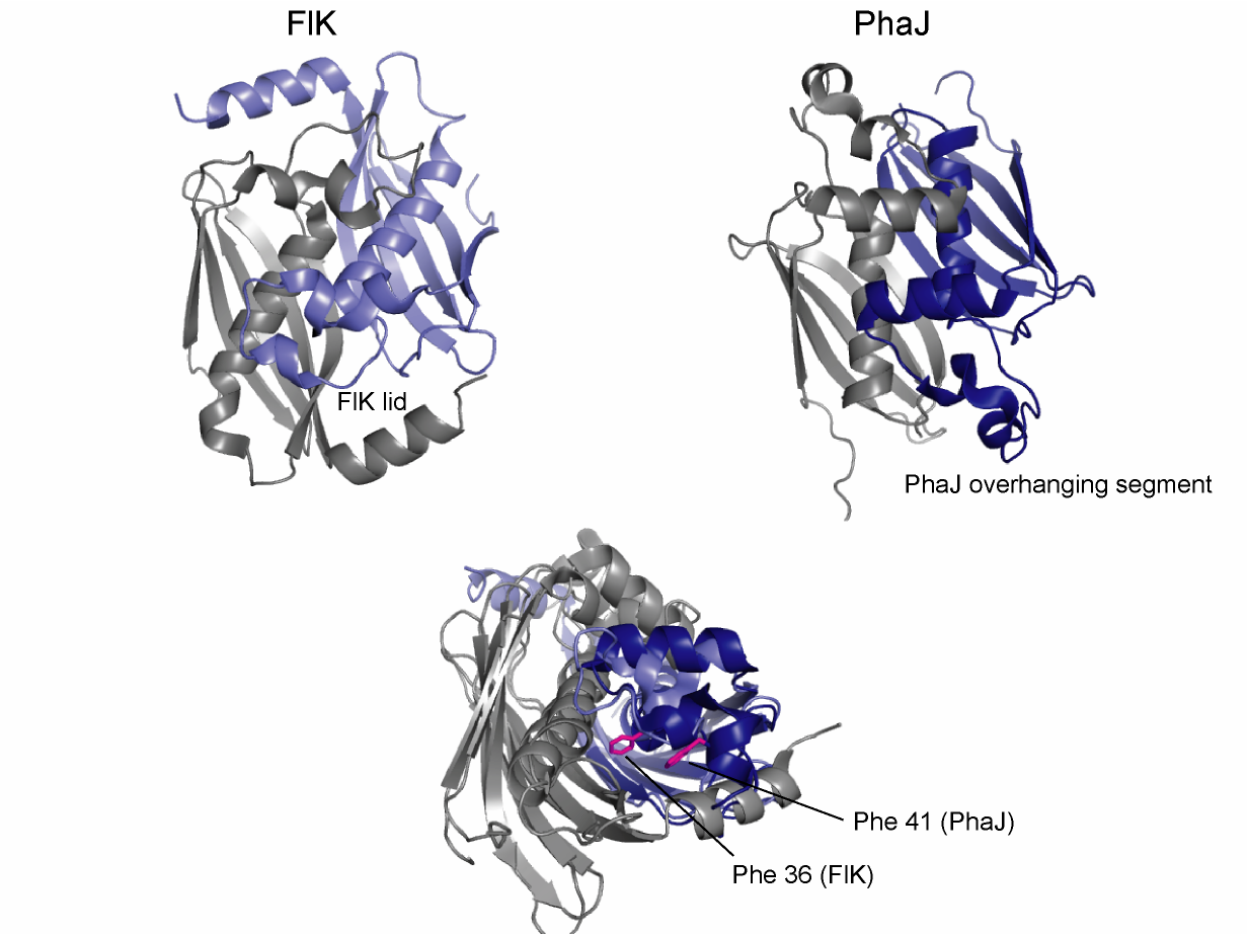

Figure S5C. Multiple sequence alignment of FlK and its closest homologs. The sequences of FlK's closest orthologs were retrieved by BLAST *(15)* searching the NCBI database. Orthologs with >50% sequence identity were aligned to FlK using MUSCLE *(16)* for sequence comparison. Residue 36 (FlK numbering) is shown in red.

```
Streptomyces cattleya                -MKDGMRVGERFTHDFVVPPHKTVRHLYPESPEFAEFPEVFATGFMVGLMEWACVRAMAP
Rhodospirillum rubrum                -MRDVLKVGMGETLSFEVPREKTVPFLYPESAEFQAIPEVFATGYMIGLMEWCCVRSLAP
Afipia sp. 1NLS2                     -MKPSLTAGSTHRFTYRVPENKTVPHLFPEARDFQIMPHVFATGYMVGLMEWACMDMIRP
Oligotropha carboxidovorans          -MKPTLVAGATHRFTYRVPENKTVPDLFPEAHDFQIMPHVFATGYMVGLMEWACMDLIRP
Hyphomicrobium sp. MC1               -MKDTLHPGAKTQFTYRVPATKTVPHLYPEAHEFQLMPTVFATGYMVGLMEWTCLHIIAP
Hyphomicrobium denitrificans         -MKPSLQAGARTEFSFRVPATKTVPYLYPEAREFQLMPTVFATGFMVGLMEWTCLHILEE
Hyphomicrobium denitrificans         -MKPSLQAGARTQFSFRVPATKTVPHLYPEAREFQLMPTVFATGFMVGLMEWTCLHIIDP
Geobacter sp. M18                    -MKDTLAAGIGTTLKFSVPVEKTVPCLYPESALFREMPEVFATGYLVGFIEWACMEALAP
Geobacter bemidjiensis               -MKE-LQVGLKHTFSYLVPKERTVPFLYPESSYFQVMPEVFATGYMVGFMEWACMDALAP
Anaeromyxobacter sp. Fw109-5         -MKSTLAPGVSLTFRYQVPETKTVPHVFPESPRFVEMPQVFATAFMVGLLEWACIEAMQP
Methanosarcina acetivorans           MDSSTLKPGLAYEFRFKIPENKTVPYLYPESPEFQVMPKVFATGFMVGLFEWACIQAINP
Desulfosporosinus youngiae           -MKSTLQSGLYYEFKFTVPENKTVPYLYPESEEFQAMPKVFGTGFMVGLFEWACIKAINP
Desulfosporosinus meridiei           -MKSTLQSGLSYEFKFTVPEDKTVPYLYPESEEFQAMPKVFGTGFMVGLFEWACIKAINP
Desulfosporosinus orientis           -MKSTLQSGLDYEFKFTVPDNKTVPYLYPEAEEFQAMPKVFGTGFMVGLFEWACIKAINP
Gallionella capsiferriformans        -MKDTLKPGIRFEHKYLVPANKTVPALYPESPEFLAMPEVFATGFMVGFLEWACIMAIKP
Sideroxydans lithotrophicus          -MKDTLKPGIRYEHRFLVPSSKTVPALYPEAEEFLAMPEVFATGFLVGFLEWACIKCINP
                                          :  *      : :*  .**  ::**:  *  :* **.*.:::*::** *:  :

Streptomyces cattleya                YLE-PGEGSLGTAICVTHTAATPPGLTVTVTAELRSVEGRRLSWRVSAHDGVDEIGSGTH
Rhodospirillum rubrum                ALE-DGEGSLGIAINVSHLAPTPPGARVVVEAKIIAIDGRKVSWHVVARDEVDLIGEGTI
Afipia sp. 1NLS2                     HLE-EGEGTLGTLINVNHTAATPPGLTIHVDVECTDVKGKLLRFNVKAHDGVDVIGEGRH
Oligotropha_carboxidovorans          HLE-DGEGTLGTLIDVNHTAATPPGLTINVDVECLEVKGKWSRFKVKAHDGIDVIGEGFH
Hyphomicrobium sp. MC1               HLD-KGEGSLGVHINVSHLAATVPGQTVTVDAECTKVAGRRLYFHVKAHDGIDLIGEGEH
Hyphomicrobium denitrificans         HLD-QGEGSLGVHINVSHVAATVPGQTVTVEAECTKVAGRRIFFHVKAHDGIDLIGEGEH
Hyphomicrobium denitrificans         HLD-PGEGSLGVHINVSHVAATVPGQTVTVEAECTKVAGRRIFFHVKAHDGIDLIGEGEH
Geobacter sp. M18                    YLE-EDERSVGTMINVTHSAATPPGMEVTAQVRCVEVTGKRTVWEIEVHDQADLISKGTH
Geobacter bemidjiensis               YLD-EGERTVGTMINVTHEAATPAGMEVTATVTLVEVDGKRTVWEIEARDEVEVIGRGRH
Anaeromyxobacter sp. Fw109-5         HLD-GGEQSVGTGIWVTHGAATPPGFTVTVDVAVTKVEGRRLTFSVRAHDGVDAICEGTH
Methanosarcina acetivorans           YLDFPAEQTVGTDVRLSHSAATPPGLTVTVKIKLEKIEGRKLTFSIIADDGVDKISEGTH
Desulfosporosinus youngiae           HLDWPNEQTVGTDVKLSHLAATPPGLTVTVKLRLEKIEGKKLFFHVEAHDGIDLISEGTH
Desulfosporosinus meridiei           HLDWPNEQTVGTDVKLSHIAATPPGFTVTVKLRLEKIEGKKLLFHVEAHDGVDQISEGTH
Desulfosporosinus orientis           HLDWPNEQTVGTDVKLSHIAATPPGFTVTVKLRLEKIDGKRLLFHVEAHDGVDLISEGTH
Gallionella capsiferriformans        HLDWPEEQSVGTHINVSHEAATPPGLEVTASVELTIVDGRRLTFAVSAHDGVDTIARGTH
Sideroxydans lithotrophicus          HIDWPAEQTVGTHINVSHQAATPPGLEVTALVELVEVDGRKLVFQVEAHDGVEVISKGRH
                                      ::   * ::*  : :.* *.* .*  : .      : *.   : : . *  : *  *

Streptomyces cattleya                ERAVIHLEKFNAKVRQKTPAG------------
Rhodospirillum rubrum                GRAVVRWSSFTQRLAEKAATIAARRATKPSGTD
Afipia sp. 1NLS                      ERYAVMWDKFTARVSKKAAKAGVAA--------
Oligotropha carboxidovorans          ERYAVMWDKFKARVSEKAVKAGVAA--------
Hyphomicrobium sp. MC1               QRMVVNWEKFEQRVNEKAKIARLAPITRGTV--
Hyphomicrobium denitrificans         ERVVVDWEKFEQRVNGKAKLARLSPITRGTG--
Hyphomicrobium denitrificans         QRMIVDWEKFEQRVNDKAKRARLSPITRGTG--
Geobacter sp. M18                    ERFTIRLEQFKSRLKTKAEAAGIIIA-------
Geobacter bemidjiensis               ERFVIDYEKFSKRVAAKGNK-------------
Anaeromyxobacter sp. Fw109-5         ERFVIDRARFDRKIQEKLAASTSC---------
Methanosarcina acetivorans           ERFIIDAAKFNSKAEAKAKNANN----------
Desulfosporosinus youngiae           ERFVIDAAKFNEKVNRKSKTESVTE--------
Desulfosporosinus meridiei           ERFIINAAKFNEKVTRKSEIKA-----------
Desulfosporosinus orientis           ERFIIDAAKFNEKVTRKSEIERITE--------
Gallionella capsiferriformans        ERYVINKEKFDNKLRDKREKINQR---------
Sideroxydans lithotrophicus          ERFIINREKFEAKIGEKMRRSDT----------
                                      *  :    *  .   *
```

Figure S6. 3,3,3-Trifluoropropionyl-CoA hydrolysis, fluoride release, and FlK inactivation. (A) Fluoride release (black) and fraction FlK activity remaining after treatment with 3,3,3-trifluoropropionyl-CoA (red). Fluoride release was monitored using a fluoride electrode. Fraction activity remaining was determined by diluting an aliquot of 3,3,3-trifluoropropionyl-CoA-treated FlK into a reaction mixture containing fluoroacetyl-CoA at various times. (B) Time course for CoA release from 3,3,3-trifluoropropionyl-CoA (1 mM) catalyzed by FlK (10 μM) as monitored using DTNB. The time course shows rapid formation of 1 equivalent of CoA, followed by a much slower rate that is identical to the background rate of uncatalyzed hydrolysis, indicating inactivation of the enzyme after one turnover. Inactivation occurs with a rate constant identical to that of CoA formation (or enzyme acylation) as the active site cannot accommodate another substrate. (C) Modified E50 peptide resulting from hydroxylamine-trapping of FlK treated with the 3,3,3-trifluoropropionyl-CoA substrate. (D) Unmodified peptide from FlK treated with hydroxylamine in the absence of an acyl-CoA substrate. (E) Kinetic scheme showing rate constants derived from plots in (A) and (B).

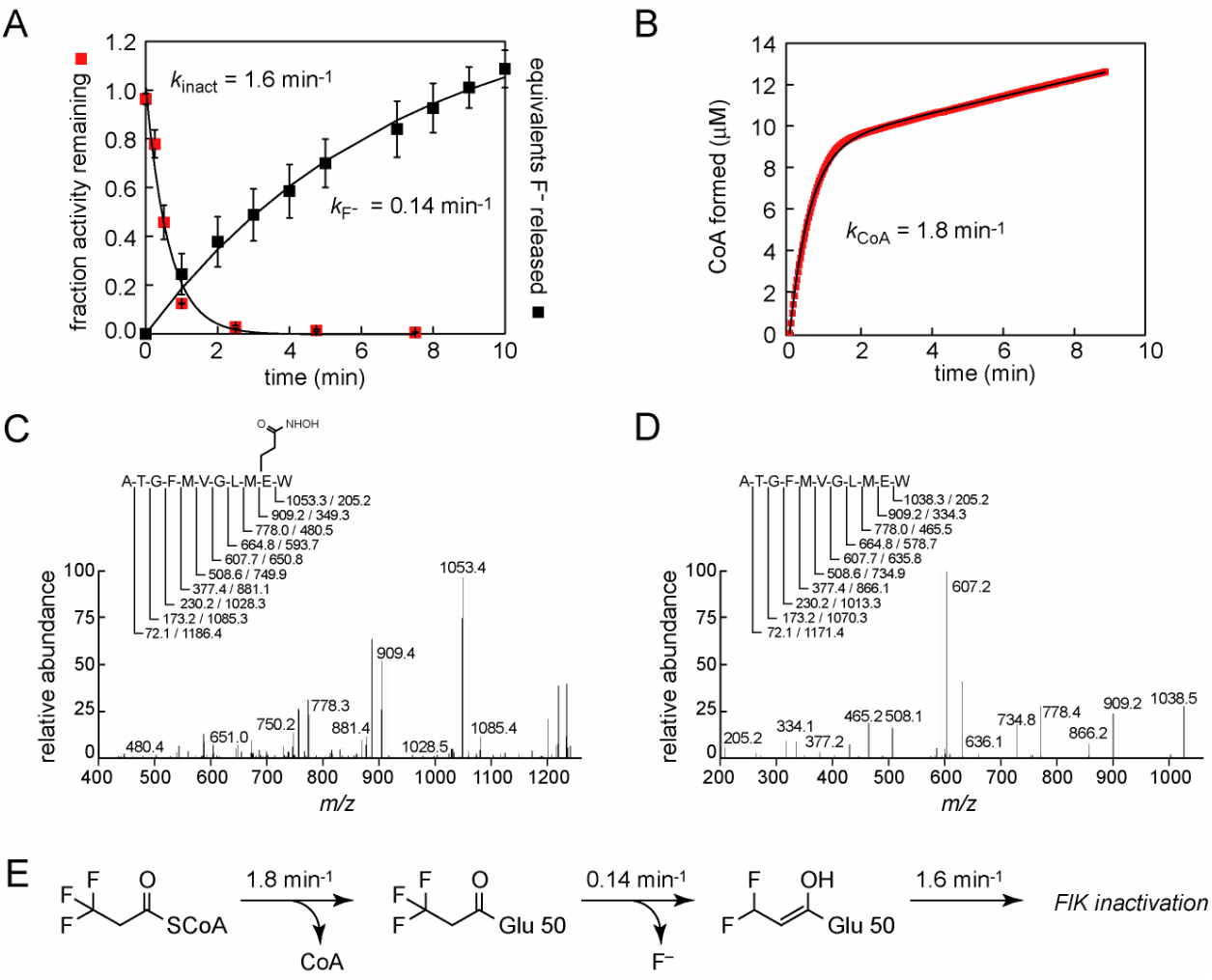

Figure S7. Pre-steady-state kinetics of [$^2H_2$]-fluoroacetyl-CoA hydrolysis by FlK. Pre-steady-state measurements show that FlK (25 μM) develops burst behavior upon hydrolysis of [$^2H_2$]-fluoroacetyl-CoA, indicating both that an acyl-enzyme intermediate is formed and that enzyme deacylation becomes partially rate-limiting, consistent with the observed KIE.

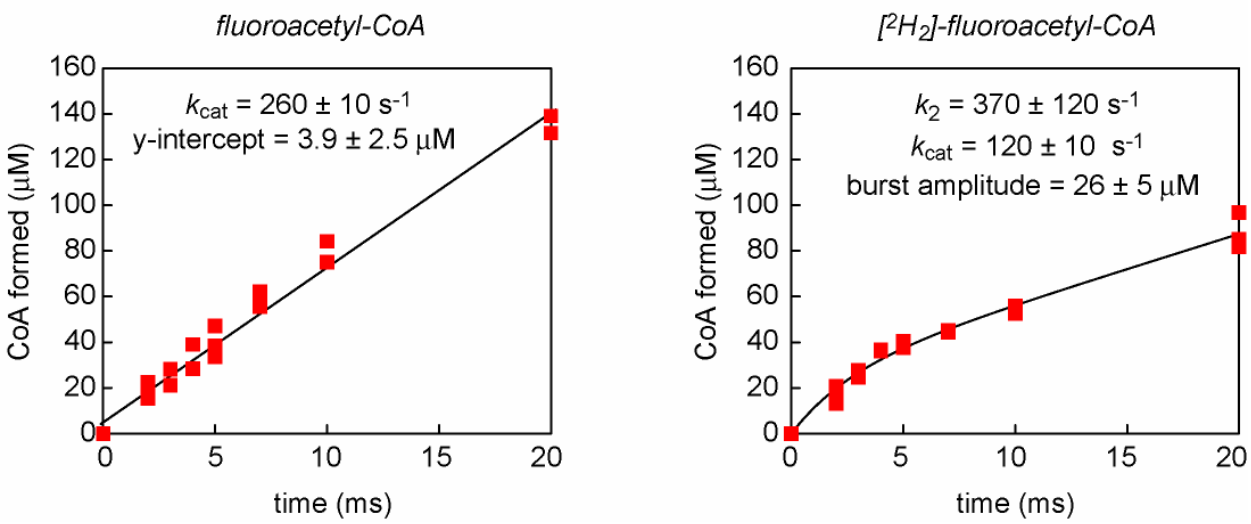

Figure S8. Characterization of FlK-H76A. (A) Michaelis-Menten curve for FlK-H76A-catalyzed hydrolysis of fluoroacetyl-CoA in the presence (black) and absence (red) of 30% (w/v) sucrose. (B) FlK-H76A-catalyzed hydrolysis of fluoroacetyl-CoA (black) and [$^2H_2$]-fluoroacetyl-CoA (red). Upon introduction of the H76A mutation, the KIE indicating C_α-deprotonation is no longer observed.

A

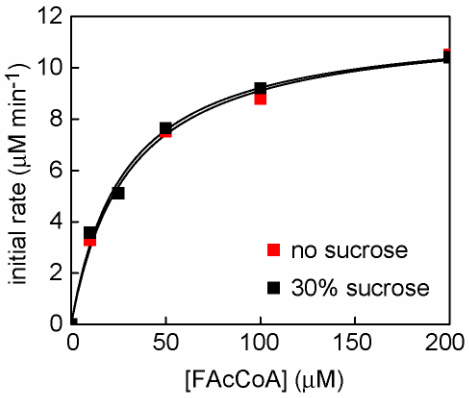

	% sucrose	k_{cat} (s^{-1})	K_M (μM)	k_{cat}/K_M ($M^{-1}s^{-1}$)
fluoroacetyl-CoA	0	0.04 ± 0.001	30 ± 4	1300 ± 200
	30	0.04 ± 0.001	28 ± 3	1300 ± 200

B

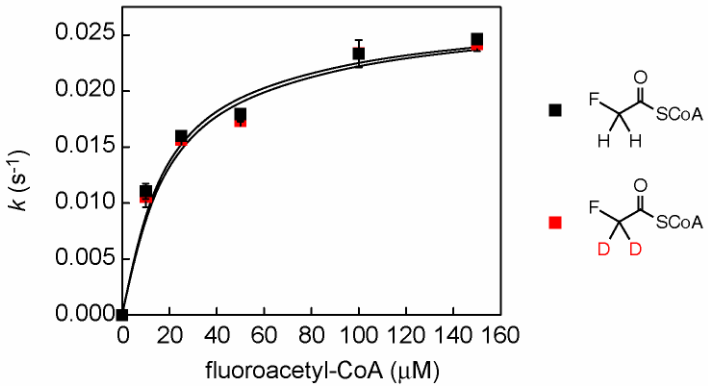

Scheme S1. Alternative mechanism for enolate breakdown. An alternative mechanism for breakdown of the anhydride enolate intermediate would involve nucleophilic attack of hydroxide or water at the carbonyl of a carbanion or enolate, both which should be slower than direct attack at a neutral anhydride as observed for acetyl-CoA based on the rates of the hydrolysis of the corresponding thioester.

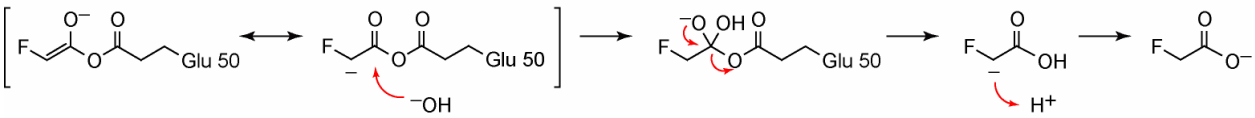

Figure S9. Quantification of exchange of α-protons with D_2O. Deuterium incorporation into fluoroacetate or acetate was analyzed by NMR following FlK-catalyzed hydrolysis of the corresponding thioester. (A) ^{19}F NMR analysis indicates that <1% of fluoroacetyl-CoA α-protons exchange with solvent as compared to a standard corresponding to 1% exchange. (B) ^{2}H NMR analysis indicates that <1% of acetyl-CoA α-protons exchange with solvent as compared to a standard corresponding to 1% exchange.

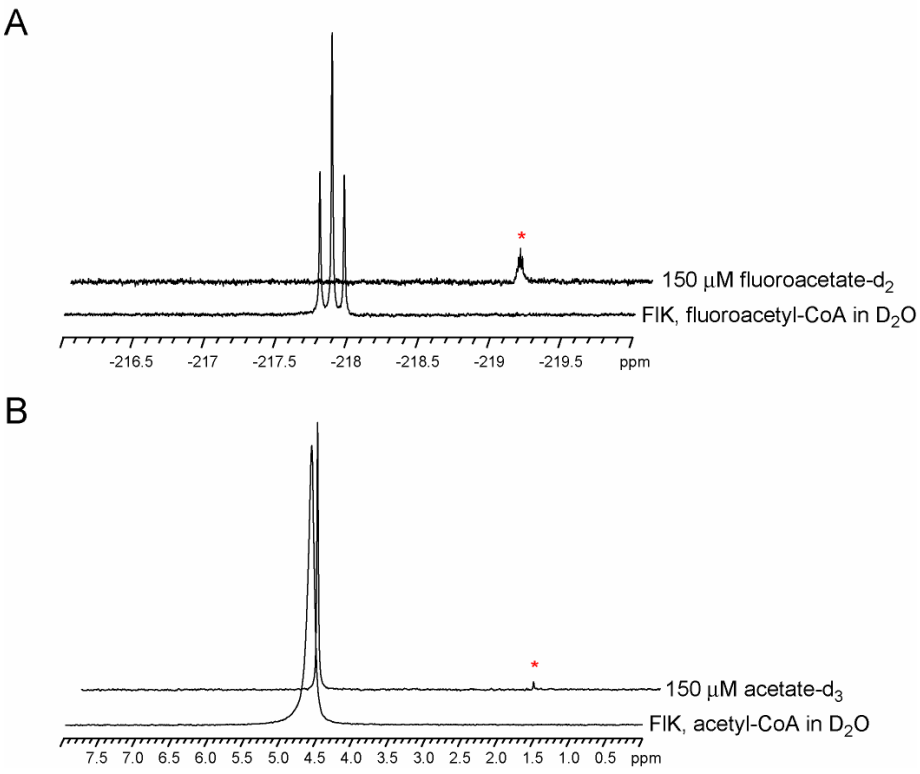

Figure S10. Characterization of acyl-CoA substrates. (A) Acyl-CoA substrates were analyzed by RP-HPLC as described for non-enzymatic hydrolysis experiments. Absorbance was monitored at 260 nm. (B) $^{1}H/^{13}C$ HMBC spectrum of fluoroacetyl-CoA. (C) $^{1}H/^{13}C$ HMBC spectrum of chloroacetyl-CoA. (D) $^{1}H/^{13}C$ HMBC spectrum of bromoacetyl-CoA. (E) $^{1}H/^{13}C$ HMBC spectrum of cyanoacetyl-CoA. $^{1}H/^{13}C$ HMBC indicates that the cyanoacetyl-CoA has a stable enolate form under these conditions. Crosspeaks corresponding to the enolate tautomer are circled. Peak 37 corresponds to the crosspeak between the α-protons and the carbon of the cyano group (see Materials and Methods for acyl-CoA numbering).

A

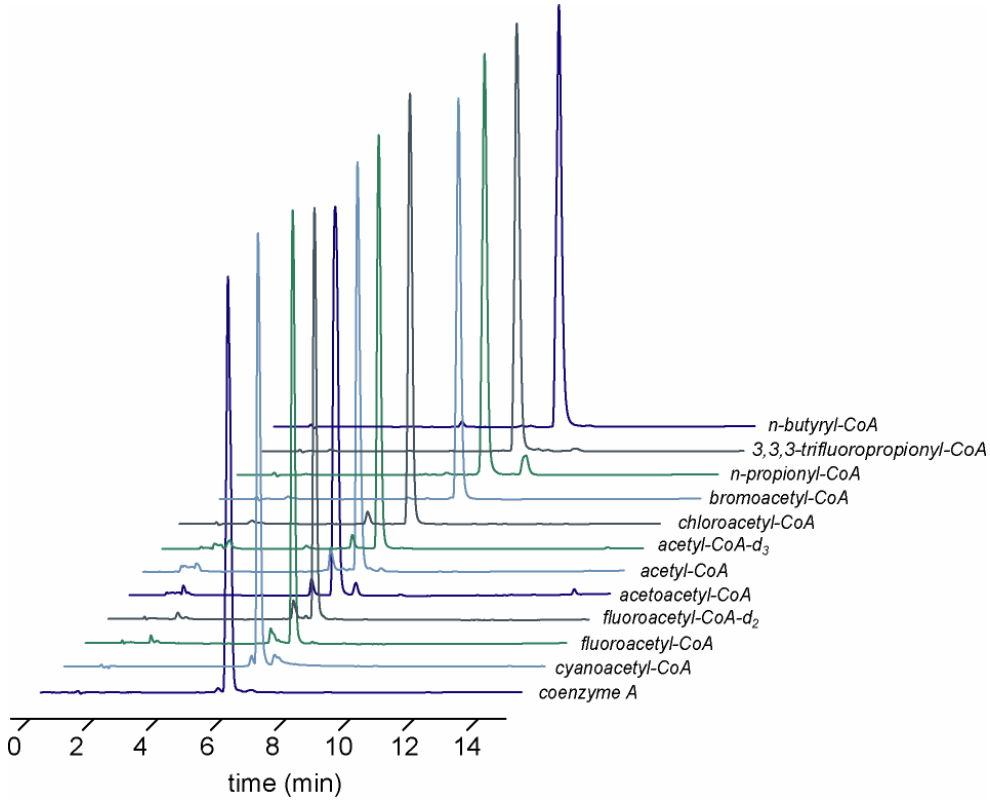

B

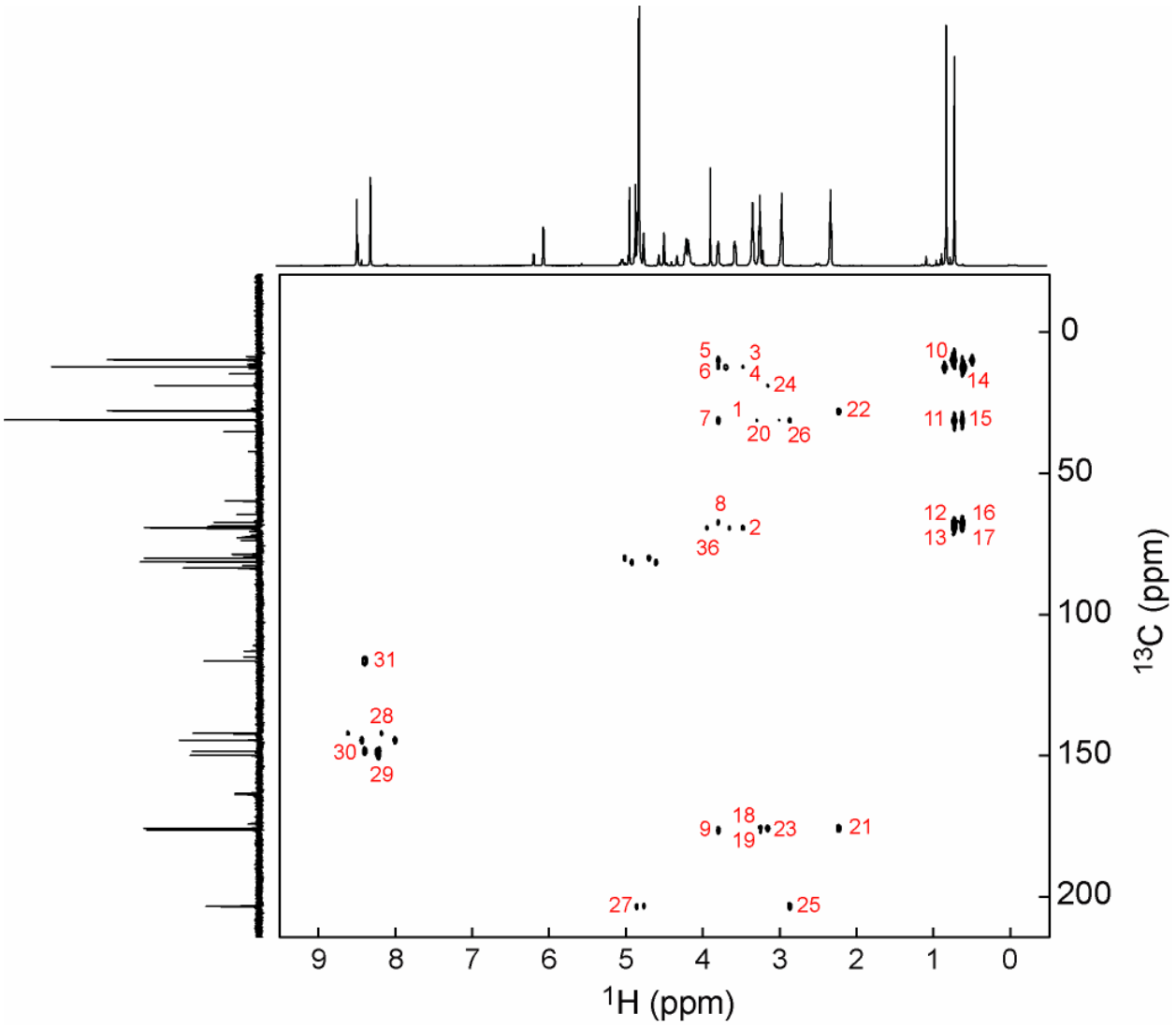
5
6
3
4
24
10
14
7
1
20
26
22
11
15
8
2
36
12
13
16
17
31
28
30
29
9
18
19
23
21
27
25
0
50
100
150
200
^{13}C (ppm)
9
8
7
6
5
4
3
2
1
0
^{1}H (ppm)

C

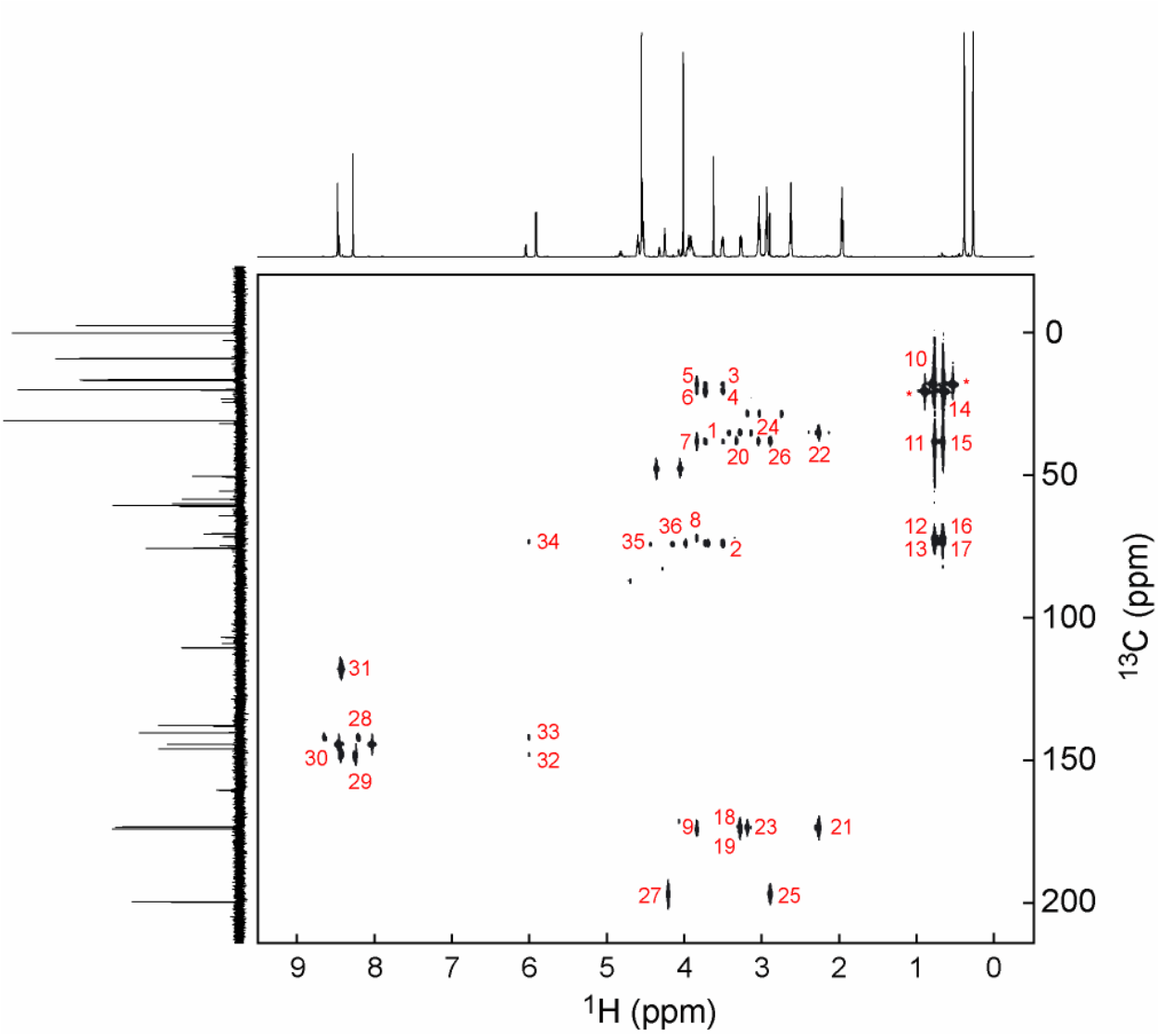
0
50
100
150
200
^{13}C (ppm)
9
8
7
6
5
4
3
2
1
0
^{1}H (ppm)
1
2
3
4
5
6
7
8
9
10
11
12
13
14
15
16
17
18
19
20
21
22
23
24
25
26
27
28
29
30
31
32
33
34
35
36

D

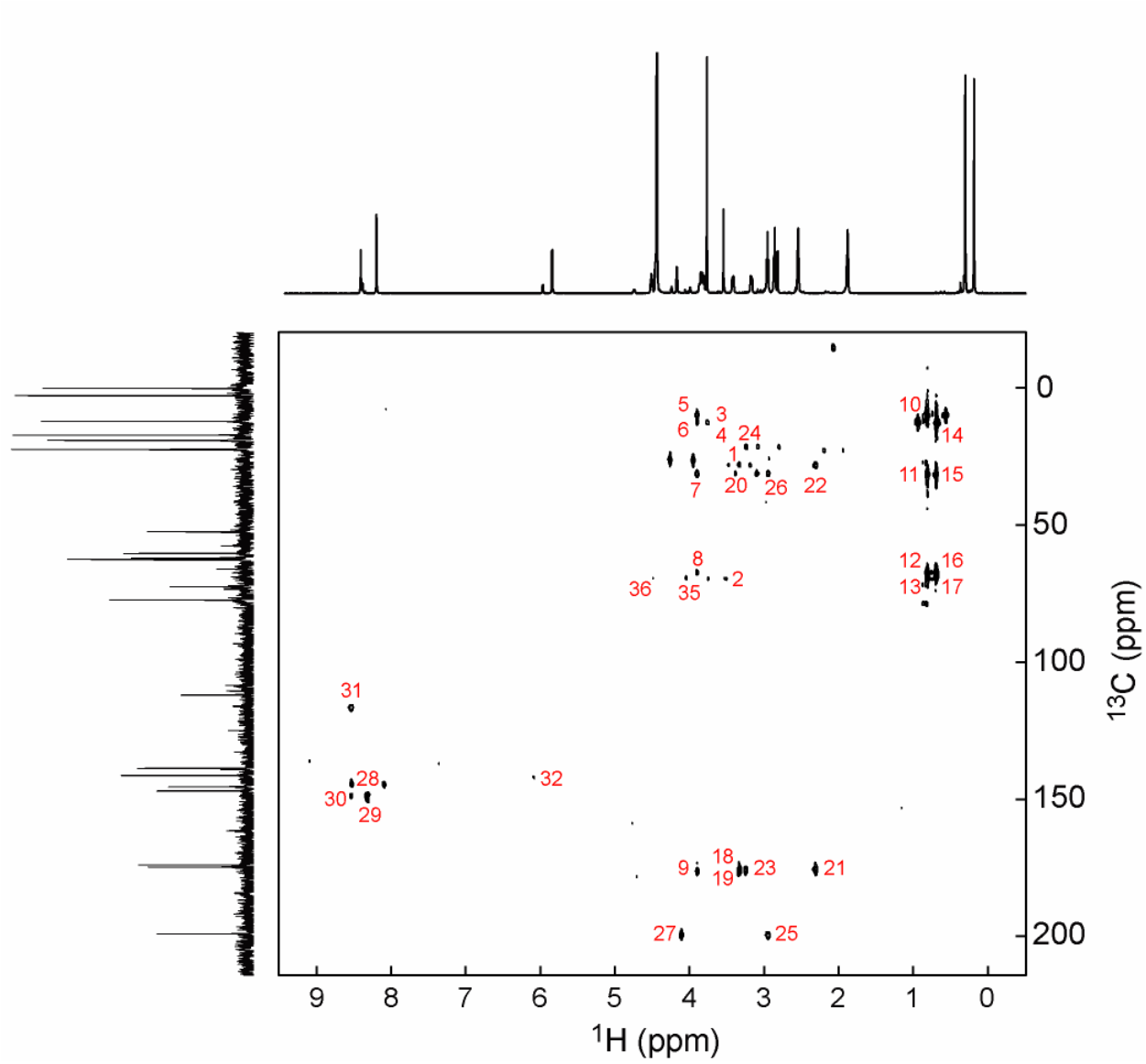
5
6
3
4
24
1
7
20
26
22
10
14
11
15
8
36
35
2
12
16
13
17
31
28
30
29
32
9
18
19
23
21
27
25
0
50
100
150
200
^{13}C (ppm)
9
8
7
6
5
4
3
2
1
0
^{1}H (ppm)

E

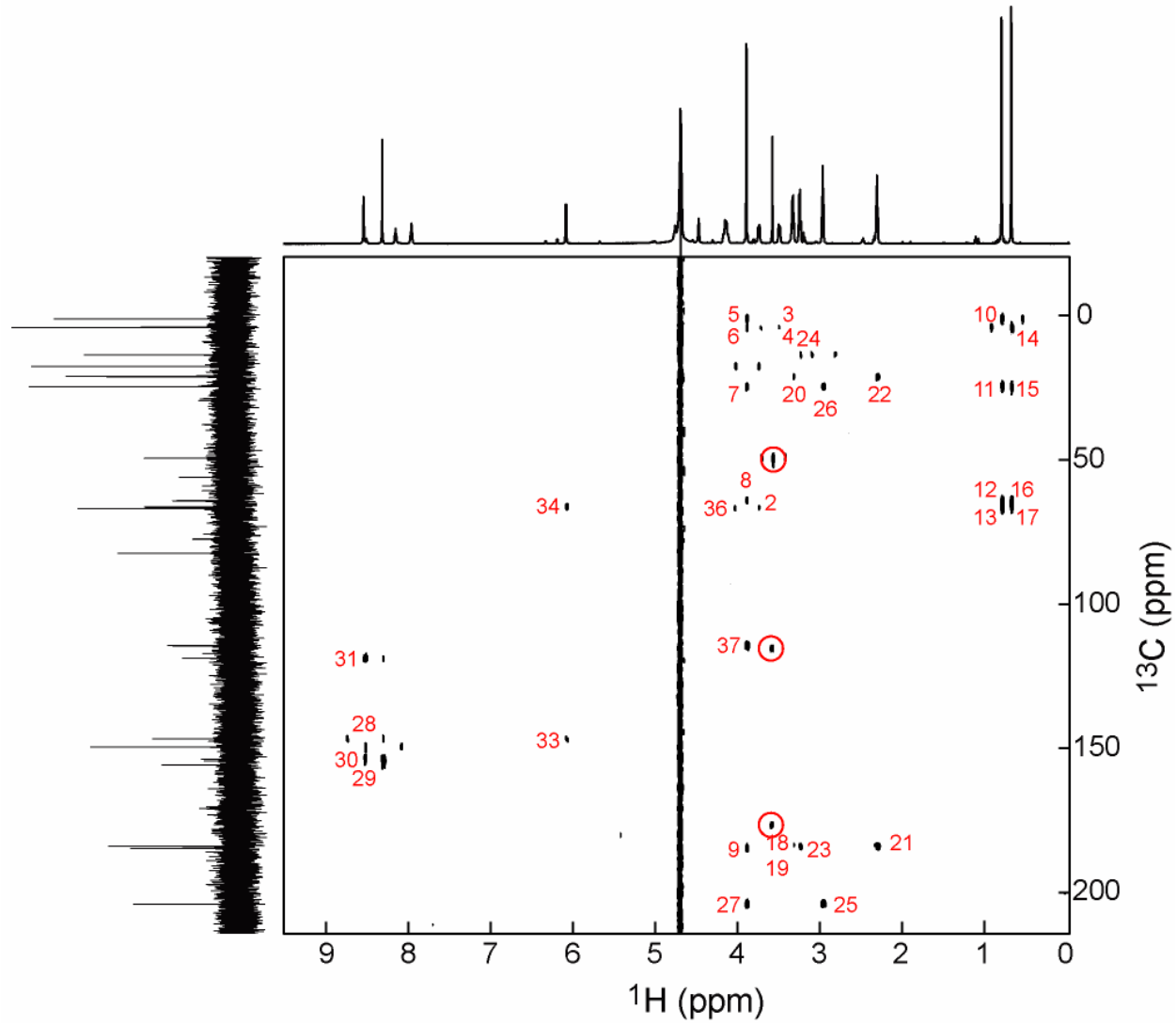
5
6
3
4
24
10
14
7
20
26
22
11
15
8
34
36
2
12
16
13
17
31
37
28
33
30
29
9
18
19
23
21
27
25
0
50
100
150
200
13C (ppm)
9
8
7
6
5
4
3
2
1
0
1H (ppm)

Literature Cited

1. Weeks, A. M., Coyle, S. M., Jinek, M., Doudna, J. A., Chang, M. C. (2010) Structural and biochemical studies of a fluoroacetyl-CoA-specific thioesterase reveal a molecular basis for fluorine selectivity. *Biochemistry* 49**:** 9269-9279.
2. Huang, F., et al. (2006) The gene cluster for fluorometabolite biosynthesis in *Streptomyces cattleya*: A thioesterase confers resistance to fluoroacetyl-coenzyme A. *Chem. Biol.* 13**:** 475-484.
3. Yu, M., de Carvalho, L. P., Sun, G., Blanchard, J. S. (2006) Activity-based substrate profiling for Gcn5-related *N*-acetyltransferases: The use of chloroacetyl-coenzyme A to identify protein substrates. *J. Am. Chem. Soc.* 128**:** 15356-15357.
4. Taft, R. W., Jr. (1952) Polar and steric substituent constants for aliphatic and *o*-benzoate groups from rates of esterification and hydrolysis of esters. *J. Am. Chem. Soc.* 74**:** 3120-3128.
5. Hansch, C., Leo, A. (1979) *Substituent Constants for Correlation Analysis in Chemistry and Biology* (Wiley, New York).
6. Eng, J. K., MacCormack, A. L., Yates, J. R., III (1994) An approach to correlated tandem mass spectral data of peptides with amino acid sequences in a protein database. *J. Am. Soc. Mass Spectrom.* 5**:** 976-989.
7. Tabb, D. L., McDonald, W. H., Yates, J. R., III (2002) DTASelect and Contrast: Tools for assembling and comparing protein identifications from shotgun proteomics. *J. Proteome Res.* 1**:** 21-26.
8. Simossis, V. A., Heringa, J. (2005) PRALINE: A multiple sequence alignment toolbox that integrates homology-extended and secondary structure information. *Nucleic Acids Res.* 33**:** W289-294.
9. Tamura, K., et al. (2011) MEGA5: Molecular evolutionary genetics analysis using maximum likelihood, evolutionary distance, and maximum parsimony methods. *Mol. Biol. Evol.* 28**:** 2731-2739.
10. Dias, M. V., et al. (2010) Structural basis for the activity and substrate specificity of fluoroacetyl-CoA thioesterase FlK. *J. Biol. Chem.* 285**:** 22495-22504.
11. Hisano, T., et al. (2003) Crystal structure of the (*R*)-specific enoyl-CoA hydratase from *Aeromonas caviae* involved in polyhydroxyalkanoate biosynthesis. *J. Biol. Chem.* 278**:** 617-624.
12. Thoden, J. B., Zhuang, Z., Dunaway-Mariano, D., Holden, H. M. (2003) The structure of 4-hydroxybenzoyl-CoA thioesterase from *Arthrobacter* sp. strain SU. *J. Biol. Chem.* 278**:** 43709-43716.
13. Cao, J., Xu, H., Zhao, H., Gong, W., Dunaway-Mariano, D. (2009) The mechanisms of human hotdog-fold thioesterase 2 (hTHEM2) substrate recognition and catalysis illuminated by a structure and function based analysis. *Biochemistry* 48**:** 1293-1304.
14. Emsley, P., Cowtan, K. (2004) Coot: Model-building tools for molecular graphics. *Acta Crystallogr. D* 60**:** 2126-2132.
15. Altschul, S. F., Gish, W., Miller, W., Myers, E. W., Lipman, D. J. (1990) Basic local alignment search tool. *J. Mol. Biol.* 215**:** 403-410.
16. Edgar, R. C. (2004) MUSCLE: Multiple sequence alignment with high accuracy and high throughput. *Nucleic Acids Res.* 32**:** 1792-1797.